Design and Improvement of Components Placement in Electric

Forklift for Ease of Maintenance and Maximizing Safety

Temesgen Gebreselasie Hailemariam

A Thesis submitted to the Department of Mechanical Engineering

School of Mechanical, Chemical and Materials Engineering

Presented in Partial Fulfillment of the Requirements for the Degree of Master's in Automotive Engineering

Office of Graduate Studies

Adama Science and Technology University

October 2023

Adama, Ethiopia

Design and Improvement of Components Placement in Electric Forklift for Ease of Maintenance and Maximizing Safety

Temesgen Gebreselasie Hailemariam

Advisor: Getachew Alemayehu (PhD)

A Thesis submitted to the Department of Mechanical Engineering

School of Mechanical, Chemical and Materials Engineering.

Presented in Partial Fulfillment of the Requirements for the Degree of Master's in Automotive Engineering

Office of Graduate Studies

Adama Science and Technology University

October 2023

Adama, Ethiopia

Declaration

I hereby declare that this Master Thesis entitled "***Design and Improvement of Components Placement in Electric Forklift for Ease of Maintenance and maximizing safety***" is my original work. That is, it has not been submitted for the award of any academic degree, diploma, or certificate in any other university. All sources of materials that are used for this thesis have been duly acknowledged through citation.

Temesgen Gebreselasie	_____	October 2023
Name of the student	Signature	Date

Recommendation

I/we, the advisor(s) of this thesis, hereby certify that I/we have read the revised version of the thesis entitled "***Design and Improvement of Components Placement in Electric Forklift for Ease of Maintenance and maximizing safety***" prepared under my/our guidance by Temesgen Gebreselasie submitted in partial fulfillment of the requirements for the degree of Master's of Science in Automotive Engineering. Therefore, I/we recommend the submission of revised version of the thesis to the department following the applicable procedures.

_____	_____	_____
Major Advisor	Signature	Date
_____	_____	_____
Co-advisor	Signature	Date

Approval

I/we, the advisors of the thesis entitled "***Design and Improvement of Components Placement in Electric Forklift for Ease of Maintenance and maximizing safety***" and developed by Temesgen Gebreselasie hereby certify that the recommendation and suggestions made by the board of examiners are appropriately incorporated into the final version of the thesis.

Major Advisor	Signature	Date
Co-advisor	Signature	Date

We, the undersigned, members of the Board of Examiners of the thesis by Temesgen Gebreselasie have read and evaluated the thesis entitled "***Design and Improvement of Components Placement in Electric Forklift for Ease of Maintenance and maximizing safety***" and examined the candidate during open defense. This is, therefore, to certify that the thesis is accepted for partial fulfillment of the requirement of the degree of Master of Science in Automotive Engineering.

Chairperson	Signature	Date
Internal Examiner	Signature	Date
External Examiner	Signature	Date

Finally, approval and acceptance of the thesis is contingent upon submission of its final copy to the Office of Postgraduate Studies (OPGS) through the Department Graduate Council (DGC) and School Graduate Committee (SGC).

Department Head	Signature	Date
School Dean	Signature	Date
Office of Postgraduate Studies, Dean	Signature	Date

Acknowledgement

I would like to express my gratitude to the almighty GOD for giving me time, strength and health during the preparation of this thesis. My deepest gratitude goes to my Advisor, Getachew Alemayehu (PhD), for his help, advice and guidance that gave me direction and made me put intelligent effort on this thesis work. My special thanks go to my family and my friends, for their unwavering support and encouragement throughout my thesis. Then, I would like to express my sincere gratitude and appreciation to my classmates.

Table of Contents

List of Table

List of Figures

Acronyms and Abbreviations

3D	-	*Three dimensional*
A	-	*Ampere, Amplitude, Area*
A_S	-	Accessibility score
AC	-	*Alternating Current*
b_w	-	Wheel base
CAD	-	*Computer Aided Design or Drafting*
Cp	-	*Specific heat at constant pressure*
d	-	*Diameter*
d_{ax}	-	Distance from front axle to load center
d_f	-	Front axle position
d_i	-	*Inner tube diameter*
d_o	-	*Outer tube diameter*
d_r	-	Rear axle position
F	-	*Correction Factor for LMTD*
h	-	*Height, heat transfer coefficient*
JIC	-	*Joint Industry Conference*
k	-	*Thermal conductivity*
Kg	-	*Kilogram*
KW	-	*Kilo Watt*
L	-	*Length*
L_t	-	*Length of a tube*
LMTD	-	*Logarithmic Mean Temperature Difference*
m	-	Mass
mm	-	*Millimeter*
$\dot{m}$	-	*Mass flow rate*
NFPA	-	*National Fluid Power Association's*
NPSHA	-	*Net Positive Suction Head Available*
NPSHR	-	*Net Positive Suction Head Required*
NTU	-	*Number of Transfer Units*
Nt	-	*Number of tubes*

Nu	-	*Nusselt Number*
P_{pm}	-	Power consumption of the pump motor
PD	-	*Positive displacement*
Pr	-	*Prandtl Number*
Q	-	*Heat duty or heat transfer rate*
Q_D	-	Heat dissipation requirements
Re	-	Reynolds Number
RPM	-	*Revolution Per Minute*
S	-	Stiffness
T	-	*Temperature*
Uo	-	*Overall heat transfer coefficient*
V	-	*Volume*
$\dot{V}$	-	*Volume flow rate*
v	-	*Velocity*
Vac	-	*Voltage (Alternating Current)*
W	-	*Weight*
w	-	*Width*
α_f	-	Angular frequency
Δ	-	*Delta type of connection*
ΔT	-	*Temperature difference*
ε	-	*Effectiveness*
ρ	-	*Density*
μ	-	Dynamic viscosity
η_{pm}	-	Efficiency of the pump motor
ב	-	Damping

Abstract

The Toyota forklifts are known for their reliability and durability. However, components such as pump motor and oil pump are only accessible after battery is removed from its compartment. Furthermore, since the components are only few centimeters from the floor and the protective device are not installed for them in addition to the unavailability for maintenance, the current placement of pump motor and oil pump of 8FBM 40 Toyota Electric Forklift makes them vulnerable to dirt and water. To address this issue, a new design and model for relocating the components of the 8FBM40 Toyota Electric Forklift have been developed. The new model focuses on relocating the pump motor unit with hydraulic pump and hydraulic tank of the forklift to the rear side of the forklift for ease of maintenance and to avoid vulnerability to external factors. The new location was selected based on factors such as accessibility, space availability, weight distribution, vibration generated, and heat dissipation and cooling requirement of the components relocated. Accordingly, the new location with 96.67% of the accessibility score is developed for relocating pump motor unit with hydraulic pump and hydraulic tank to the rear side of the forklift by removing few weights of the counterweight. Moreover, to increase the lifespan of the hydraulic oil and to reduce the operational cost of the forklift, in addition to relocating the pump motor unit and hydraulic tank, oil cooler is incorporated to the new design. Furthermore, the ANSYS result indicates that, the new model outperforms the current model in terms of accessibility for maintenance and structural performance. Its superior rigidity and stability, coupled with its resistance to deformation and fatigue, make it a safer and more reliable choice.

Keywords: *8FBM40, Accessibility, Availability, Forklifts, Weight Distribution*

Chapter One

1. Introduction

1.1. Background

The forklift is a versatile material handling equipment that has been around for over a century and has revolutionized the way material is handled in various industries (Vignesh et al., 2019). The first forklift was invented in 1917 by Raymond Pallet, primarily powered by gasoline engines (Conger, 2023a). They are used in a wide variety of industries to lift, load, transport, and unload heavy objects. Forklifts have significantly increased productivity, improved safety, and reduced manual labor requirements in warehouses, factories, and other workplaces (Sachin et al., 2014).

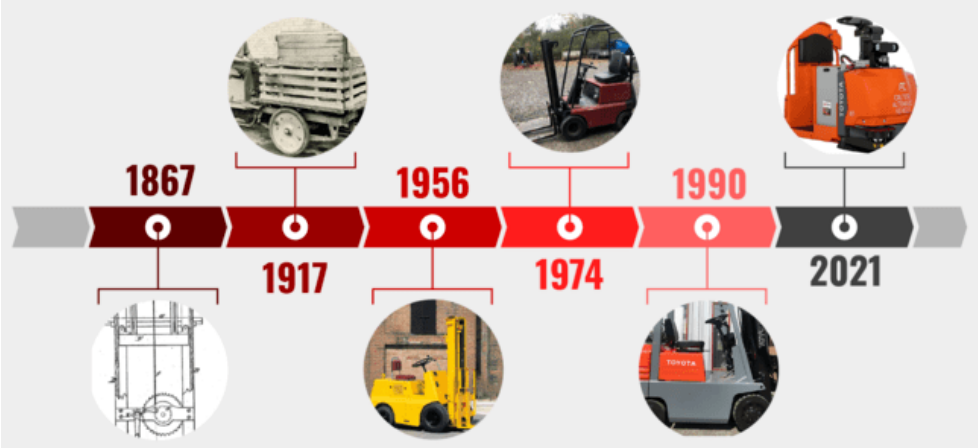

Figure 1.1: Historical developments of Forklifts (Conger, 2023a)

Conventional forklifts powered by internal combustion engines have some inherent disadvantages, such as high noise levels, emissions, and maintenance costs. These drawbacks, along with the growing need for more sustainable and environmentally friendly alternatives, led to the development of electric forklifts. Electric forklifts offer several advantages over conventional counterparts, including reduced noise levels, zero emissions,

lower operating costs, improved energy efficiency, and reduced maintenance requirements (Raut Shubham B et al., 2020).

Various manufacturers produce electric forklifts, including Toyota, Mitsubishi, Caterpillar, and Hyster, to mention a few. Toyota's electric forklifts are among the most sought-after for their durability, reliability, and efficient performance. These companies offer a wide range of electric forklift models with varying capacities and features to meet the diverse needs of industries (Toyota, 2023).

Figure 1.2: Typical Toyota electric forklifts (Toyota, 2023)

Even though electric forklifts are advantageous than conventional forklifts, however, they are vulnerable to external factors such as dust and debris, water and extreme temperatures. External factors significantly impact the performance and lifespan of electric forklifts (Ma, 2011). For instance, extreme weather conditions, such as high temperatures or cold weather, can damage the electrical components of an electric forklift; dust and dirt can get into the electrical components of an electric forklift and cause them to malfunction; water can damage the electrical components of an electric forklift and cause them to short circuit

(Massone & Boeri, 2010). These factors may cause damage to various parts of the electric forklift, leading to operational inefficiencies, increased maintenance costs, and ultimately, reducing the lifespan of the forklift.

Several parts of electric forklifts are susceptible to the effects of external factors. These include batteries, electrical components, motors, wiring, circuit boards, seals, bearings, wheels, tires, and other moving parts (Summit Toyotalift, 2023). Contamination, accumulation of dirt, moisture ingress, and corrosion can undermine their functionality and longevity. As a result, it is essential to identify the vulnerable parts and suggest possible design improvements to mitigate the effects of external factors.

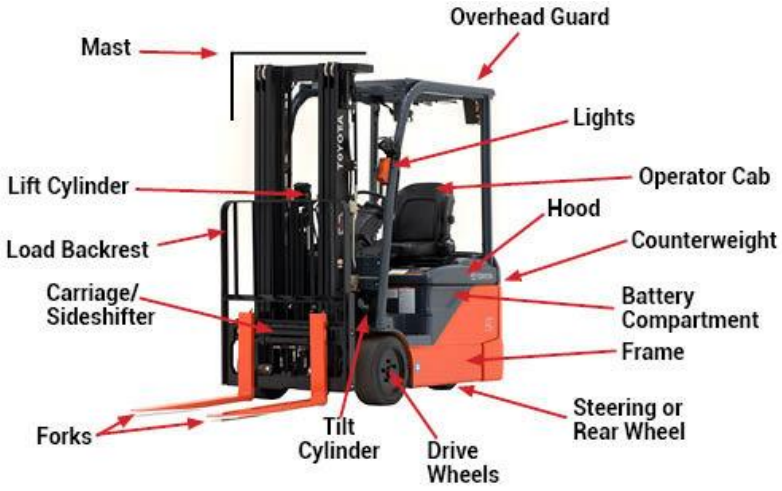

Figure 1.3: Various components of Toyota electric forklift (Summit Toyotalift, 2023)

By identifying the design and improvement areas vulnerable to external factors, it is possible to develop more resilient and efficient electric forklifts that can withstand harsh weather conditions and accidental collisions. These may include enhanced sealing mechanisms, improved insulation, anti-corrosion coatings, durable materials, intelligent sensors, and advanced filtration systems (Sachin et al., 2014). However, when considering design improvements, it is crucial to strike a balance between robustness, cost-effectiveness, and practicality (Vignesh et al., 2019). A comprehensive analysis of the specific external factors

affecting forklift operations is necessary to identify the most suitable design enhancements (Raut Shubham B et al., 2020). Thus, this study focuses on the design and improvement areas of electric forklift parts that are susceptible to external factors, with a specific emphasis on the case of Toyota forklifts. The aim of the study is to identify the external factors that pose vulnerability to Toyota electric forklift parts, as well as the design vulnerabilities of these parts that make them susceptible to these factors. The study will also develop design improvements that will make Toyota forklift parts more resistant to the effects of external factors.

1.2. Problem Statement

Toyota forklifts are some of the most popular and reliable electric forklifts on the market. They are mainly used in warehouses, food, beverage, bottling and alcohol industries. They are pollution and noise free. However, they are vulnerable to external factors such as dust and debris, water and extreme temperatures. Moreover, they are very sensitive. Hence, they need better handling and care. Due to this, they are usually utilized for indoor service only. However, in Ethiopia, most of the times they are used as a conventional type of forklift, and are utilized for outdoor also. This make various components of the forklift vulnerable to damage caused by external factors. Components such as pump motor and oil pump are only accessible after battery is removed from its compartment. Furthermore, since the components are only few centimeters from the floor and the protective device are not installed for them in addition to the unavailability for maintenance, the current placement of pump motor and oil pump of 8FBM 40 Toyota Electric Forklift makes them vulnerable to dirt and water. Thus, it is required to comprehensively analyze and modify the weak points in the design of electric forklift parts that make them susceptible to external factors. This thesis aims at design and improvement of components placement in electric forklift for the ease of maintenance and avoiding vulnerability to external factors: the case of Toyota forklift.

Figure 1.4: Electric forklift parts vulnerable to external factors

1.3. Research Question

This thesis is focused on the following research questions:

- What are the external factors that pose vulnerability to Toyota electric forklift parts?
- What are the design vulnerabilities of Toyota electric forklift parts most susceptible to external factors?
- What potential improvements can be made to the design of electric forklift parts to enhance their resistance to external factors?

1.4. Objective

1.1.1. General Objective

The general objective of this thesis is Design and Improvement of Components Placement in Electric Forklift for Ease of Maintenance and maximizing safety.

1.1.2. Specific Objectives

The specific objectives of this thesis are:

- To determine the external factors that pose vulnerability to Toyota electric forklift parts.
- To determine the design vulnerabilities of Toyota electric forklift parts most susceptible to external factors.
- To develop design and improvement of components placement that will make Toyota forklift parts more resistant to the effects of external factors.

1.5. Scope of the study

The study focuses specifically on Toyota Electric Forklifts (8FBM 40) and aims to investigate the relationship between external factors and the design vulnerabilities of electric forklift components to these external factors. It aims to provide insights into potential improvements that can be made to enhance the durability and resilience of these parts against external factors. The study is limited to the design and software model. That is, manufacturing or fabrication of the machine is not included in this thesis.

1.6. Significance of the Study

The significance of this study lies in its ability to identify the external factors that make the forklift parts vulnerable. The study will help in the development of design improvements that will make these parts more resistant to environmental factors such as weather, rough terrains, and other external factors. Furthermore, the study will help Toyota in creating a more durable and reliable electric forklift, which will increase its efficiency, safety, and minimize downtime due to parts failure. The study's results will also contribute to the development of a more sustainable and environmentally friendly forklift that minimizes its impact on the environment by reducing its vulnerability to environmental factors that can lead to early disposal.

1.7. Expected outcome

The study is expected to identify the external factors that pose vulnerability to Toyota electric forklift parts, as well as the design vulnerabilities of these parts that make them susceptible to these factors. The study will also develop design improvements that will make Toyota forklift parts more resistant to the effects of external factors.

1.8. Organization of the thesis

This thesis work is divided into seven chapters. The first chapter serves as an introduction, providing background information on Toyota electric forklift. It covers the advantage and disadvantages of this forklift. Moreover, it introduces the problem statement, study objectives, scope, expected outcome, and thesis structure. Whereas, the second chapter of the thesis reviews various types of forklifts including their design difference and application areas. It also includes the limitation of these various types of forklifts. In addition, the identified research gap is included in this chapter.

In chapter three, the materials, tools, and methods used for the research are explained. A flow chart is also provided to show the working pattern and flow of the thesis. This chapter offers a detailed description of the steps taken to complete this thesis.

Chapter four of the thesis explores the design improvements of Toyota electric forklift components that are vulnerable to external factors. Whereas, the fifth chapter of the thesis discusses the results of chapter four. It presents the findings through charts and tables. And, finally, the sixth chapter of the thesis presents conclusions and recommendations based on the insights gained from chapter six. In addition, a list of references and appendices that contain additional information are included in the document of this thesis.

Chapter Two

2. Literature Review

2.1. Overview of electric forklift design and components

A forklift is a small vehicle commonly used in large-scale industrial settings. It operates with the help of electrical and hydraulic systems and features a forked platform attached at the front (Y. Wang et al., 2016). Forklifts are predominantly found in warehouses, distribution centers, and large storage facilities where they assist in loading and unloading goods, as well as moving, stacking, and picking items (Yadav et al., 2022). They have significant importance in industries such as construction for moving heavy materials efficiently (Raut Shubham B et al., 2020). Additionally, forklifts can be enhanced with different attachments to perform tasks like sweeping, snowplowing, and facilitating training for drivers and mechanics (Toyota, 2022).

Electric forklifts are widely used in material handling operations due to their efficiency, low emissions, and quiet operation (Lototskyy et al., 2018). They differ from traditional forklifts by using rechargeable batteries to power an electric motor. The main components of an electric forklift include the chassis, battery system, electric motor, controller, and hydraulic system (Y. Wang et al., 2016). The functions of the main components are discussed below (Sachin et al., 2014):

2.1.1. Electrical Components

Electrical forklifts consist of the following major electrical system components:

- Drive Motor: - is a device that converts electro-chemical energy, provided by an industrial battery, into mechanical energy. The electric motor converts electrical energy from the battery into mechanical energy, enabling the movement of the forklift.

- The controller regulates voltage supply, ensuring safe operation, managing energy regeneration during braking, and controlling acceleration, speed, and braking for smooth operation.
- Pump motor: - it is a combination stator coil & rotor, coupled with spline to hydraulic pump to provide mechanical energy.
- Traction logic: - is an electrical component used for controlling the driving mechanism & linked with U, V, W cable drive motor.
- Lifting logic: - is an electrical device used to control working condition of pump motor.
- DC to DC Convertor: - is used to convert 80V DC to 24 V DC and 24V an input voltage for horn, lighting, display board, arm rest card, fuse board, buzzer & MCB.
- Master Cardboard (MCB)- monitors over all activities of the system.
- Display board - all system parameters set on the display board and if there is any failure on the FLT an error cod or symbols related with the failure will appears here.
- Arm rest card- controls the working condition of Joysticks (min levers)
- Battery: - is the main power source of the forklift, consisting of multiple lead-acid or lithium-ion batteries that provide energy for efficient operation
- SAS: - system of Active stability
- Sensors- like temperature sensor, Drive & pump motor RPM sensor, steering Angle sensor (potentiometer) accelerator potentiometer, Hight sensor, tilt angle sensor etc.

2.1.2. Mechanical Components

Electrical forklifts consist of the following major Mechanical system components:

- The chassis, typically made of steel, acts as the foundation of an electric forklift, providing stability and strength to support its load capacity.
- Mast: - is the mechanical structure on a forklift that performs the action of raising loads to the necessary required heights. It consists of a fork and an elevation

mechanism which lifts a load by hydraulic displacement and can be lowered by the natural forces of gravity.

- Pallet handler: - is a device can handle two pallets at a time.
- Rear Axle Assembly: - it consists of ram cylinder, steering arm, king pin, spindle shaft, wheel hub & bearing.
- Driver Seat: - is designed such a way that he can reach vehicle control with clear vision.
- Lifting chain: - There are many functions of the lifting chain. The most important one is as a medium between the lifting machinery and the lifting object.
- Wheel & tire: - Tires are an essential part of a car's suspension and steering system. They transmit braking and steering forces to the road surface as the car is driven and support its weight as well.

2.1.3. Hydraulic System components

Electrical forklifts consist of the following major Hydraulic System components:

- Hydraulic pump: - is a mechanical source of power that converts mechanical power into hydraulic energy (hydrostatic energy i.e., flow, pressure)
- Hydraulic hose: - they convey high-pressure oils or water between the fluid ports of the pumps and actuators,
- Oil pressure pipelines: - is a type of pipeline that is used to use in conveying hydraulic oil, at very high pressure.
- Hydraulic oil tank: - Beyond its most rudimentary role of providing fluid storage, the main functions of the hydraulic tank are to dissipate heat and allow contaminants to settle out of the fluid.
- Hydraulic oil filter: - is a component within a hydraulic system that removes damaging particulates by forcing hydraulic fluid through a porous filter element.

- Oil Control valve: - it can control the speed of an actuator in the system. The flow rate is also responsible for determining the rate of energy transfer at any specific level of pressure
- Ram cylinder: - Ram type hydraulic cylinders are the simplest type of hydraulic actuator. A ram cylinder is a hydraulic cylinder that acts as a ram.
- Steering valve: - Also known as Orbital Valves, steering control valves precisely meter the flow of pressurized steering fluid into steering cylinder or ram.
- Steering Wheel: - it controls the direction of a vehicle & it converts rotational commands of the driver into swiveling movements of the vehicle's front wheels.
- Lifting Cylinder- are actuation devices that use pressurized hydraulic fluid to produce linear motion and force. They are used in a variety of power transfer applications and can be single or double action. A single action hydraulic cylinder is pressurized for motion in only one direction, whereas a double action hydraulic cylinder can move along the horizontal (x-axis) plane, the vertical (y-axis) plane, or along any other plane of motion.

2.2. External factors affecting components of electric forklift

External factors such as environmental conditions and operational challenges significantly impact the performance and longevity of electric forklift parts. According to a study by (Carvalhal, 2020), external factors that can damage electric forklift parts include dust, dirt, moisture, extreme temperatures, and impact. They can adversely affect the components of an electric forklift.

2.2.1. Temperature

One major environmental condition that can affect electric forklift parts is temperature. High temperatures can cause various components to expand, increasing the wear and tear of moving parts. Alternatively, low temperatures can cause the fluid in the battery to thicken, lowering the battery's overall performance. Thus, operating electric forklifts in extreme temperatures can impact the longevity and effectiveness of their components (Tim O’Brien,

2020). Moreover, according to a study conducted by (Z. Yao et al., 2022), exposure to high temperatures can accelerate the degradation of key parts like batteries and electronic circuits, leading to a shorter lifespan and decreased efficiency.

2.2.2. Humidity

Another crucial environmental condition is humidity. Electric forklifts play a crucial role in various industries, including food processing or pharmaceuticals, which require specific environmental conditions. In these industries, high humidity could cause accelerated corrosion of electrical parts, leading to equipment failure (Doyle, 2021). Exposure to high levels of moisture can lead to rusting, corrosion, and short circuits. A study conducted by (Suryoputro et al., 2019) examined the impact of moisture on electric forklift battery compartments. The research found that prolonged exposure to moisture led to a decrease in battery performance, limiting the overall efficiency and lifespan of the forklifts. This demonstrates the need for proper storage and protection from moisture to prevent damage to electric forklift components.

Similarly, (Wafirulhadi et al., 2021) found that exposure to moisture and extreme temperatures resulted in corrosion, reduced performance, and increased repair costs. The authors suggested the use of suitable coatings, insulation, and temperature control systems to mitigate the impact of moisture and extreme temperatures on electric forklift parts.

2.2.3. Dust and Contaminants

Exposure to dust, chemicals, and other contaminants can severely affect electric forklift parts. These factors can damage electrical components and impair the performance of equipment. A research by (Carvalhal, 2020) highlights how prolonged exposure to dusty and dirty environments can cause clogging and damage to filters and cooling systems, resulting in decreased airflow and increased overheating risks.

In addition, a research conducted by the Occupational Safety and Health Administration (OSHA) reveals that excessive dust in a warehouse environment can infiltrate electric forklift

components, such as motors and circuitry, leading to performance degradation and potential malfunctions (OSHA, 2018). Moreover, a study conducted by (Z. Yao et al., 2022) revealed that dust and dirt in the hydraulic system of an electric forklift contributed to wear and tear, reduced efficiency, and increased maintenance costs.

2.2.4. Operational Challenges

Operational challenges also play a significant role in affecting electric forklift parts. The constant use of forklifts in demanding operational environments can subject the parts to excessive wear and tear. Research by (W. Yao et al., 2015) suggests that factors such as heavy loads, improper handling techniques, and inadequate maintenance can lead to premature failure of components like gears, bearings, and hydraulic systems. Furthermore, excessive shock and vibration during lifting and movement operations can result in loosened connections, misalignments, and fatigue failure of structural parts, as discussed in the work of (Pachakawade et al., 2018)

2.3. Electric forklift parts that are vulnerable to external factors

Various components of electric forklift may be vulnerable to external factors such as dust, temperature, humidity, and so on. Electric forklifts are vulnerable to external factors that can damage specific components, such as the battery, motor, control system, and frame. The most common components vulnerable to external factors are discussed below.

2.3.1. Battery

The battery is a critical component of an electric forklift, providing the necessary power for its operation. External factors such as extreme temperatures, improper charging techniques, and over-discharging can significantly impact battery life. For instance, high temperatures can reduce battery life, which increases the frequency of replacement needed (Volland, 2021). Moreover, according to a study conducted by (Shanghai Electric Power Company, 2019), battery health and performance deteriorate rapidly under extreme temperatures, reducing their lifespan by up to 50%.

2.3.2. Motor

The electric motor in forklifts is another essential component that is vulnerable to external factors. Dust, dirt, and debris can accumulate in the motor, leading to increased friction and reduced efficiency. A comprehensive study by the (University of Southern California, 2010) found that 60% of motor failures in electric forklifts were due to inadequate maintenance and irregular cleaning.

2.3.3. Control System

The control system of an electric forklift encompasses various electronic components responsible for monitoring and regulating its operations. External factors such as power surges, voltage fluctuations, and electromagnetic interference can disrupt the control system, leading to malfunctions and safety hazards. A report by the (Occupational Safety and Health Administration (OSHA), 1999) analyzes several accidents caused by control system failures, emphasizing the importance of periodic inspections and protection against electrical disturbances to maintain optimal performance and prevent accidents.

2.3.4. Frame

The frame of an electric forklift provides structural integrity and supports the weight it carries. External factors like collisions, overloading, and rough terrain can cause stress and damage to the frame, compromising its strength and stability. A case study by (Hyster-Yale Materials Handling, 2021) indicated that the frame of electric forklifts, which provides structural support and balance, is also vulnerable to external factors. Impact forces, such as those from collisions or heavy loads, can damage the frame and reduce the stability and safety of electric forklifts.

2.3.5. Toyota forklift design and vulnerability to external factors

The design of Toyota forklifts plays a crucial role in their performance and vulnerability to various external factors. According to (Toyota, 2022), environmental conditions, operator

training and experience can still affect their performance. Battery systems, drive motors, control systems, and braking systems are among the key areas that require proactive monitoring and maintenance. Toyota needs to incorporate moisture-proof and dust-proof construction in the design of electrical systems to prevent electrical malfunction, regulate the battery temperature, and incorporate voltage stabilizing measures in the forklift's design, according to (Cheng et al., 2021) and (Zhao et al., 2017). Electric forklifts have unique vulnerabilities that must be identified to enhance their efficiency and longevity.

2.4. Possible solutions for enhancing vulnerable parts in electric forklifts

(W. Yao et al., 2015) have studied electric forklifts from seven different manufacturers. The study found that electric forklifts from three manufacturers exhibited severe damage in collisions and falls, while the remaining forklifts showed minor damage. This suggests that the design of some electric forklifts is not as robust as others. Another study by (Lototskyy et al., 2018) found that electric forklifts from two manufacturers experienced significant battery capacity loss under freezing conditions, while the other two maintained their battery levels. This suggests that the design of some electric forklifts is not as well-suited for cold weather conditions.

In order to enhance the vulnerable parts in electric forklifts, there are a number of strategies that can be used to improve the design of electric forklifts against external threats. These include:

- The use of ruggedized components that can withstand impact and vibration.
- The use of protective guards and covers to protect vulnerable parts from damage.
- The use of environmental control systems to maintain the performance of batteries in cold weather conditions.
- The use of shock-absorbing materials and improved structural designs to enhance the resilience of vulnerable parts.
- The effective placement of components to improve the performance and longevity of electric forklift parts.

- The use of corrosion-resistant materials to protect electric forklift parts from environmental factors.

(Jönsson, 2005) evaluated the retrofitting of electric forklifts with a collision avoidance system and found that the system reduced the frequency and severity of collisions, consequently reducing repair costs and downtime. The use of corrosion-resistant materials is also important for the reliability of electric forklifts (Borgioli et al., 2018). In some industrial settings, the environment is corrosive, which can damage the components of an electric forklift. By using corrosion-resistant materials, engineers can protect these components from damage and extend the lifespan of electric forklifts. (Wu et al., 2021) highlighted the use of shock-absorbing materials and improved structural designs to enhance the resilience of vulnerable parts. Moreover, the placement of the induction motor, inverter, and power module can impact the performance of an electric forklift. By carefully considering the placement of these components, engineers can improve the performance and longevity of electric forklifts.

Improved design has had a significant impact on the reliability and safety of electric forklifts, leading to reduced downtime, increased safety ratings, and lower maintenance costs. A study conducted by (J. Wang et al., 2010) investigated the effects of design enhancements in electric forklifts and found that these improvements resulted in a considerable reduction in downtime. Furthermore, improved design has shown to significantly enhance the safety ratings of electric forklifts (Pachakawade et al., 2018). In addition to improved reliability and safety, the implementation of advanced design techniques has also resulted in lower maintenance costs for electric forklifts (Shao, 2015).

2.5. Research gap

While Toyota and other manufacturers of material handling equipment have made significant improvements in designing and improving battery-operated forklift parts, there are still research gaps that need to be addressed. Some of the research gaps on designing and improving battery-operated forklift parts that are vulnerable to external factors, in the case of

Toyota forklift, may include. Understanding the specific impact of external factors on forklift parts While it is known that external factors such as extreme temperatures, humidity, shock and vibration, dust and debris, and uneven surfaces can impact forklift parts, the specific mechanisms and extent of this impact are not fully understood and also there is no any hydraulic oil cooling mechanism. In this thesis, an attempt is made to change the existing location of components which are vulnerable to external influence and designing oil cooler for the hydraulic system with modifying and design the new location.

Chapter Three

3. Methodology

For the ease of maintenance and avoiding vulnerability to external factors of Toyota electric forklift, design and improvement of components placement was performed. The design emphasizes the improvement of the location of the pump motor units. The methodology for design and modeling can be broken down into several steps. The key procedures followed in this study are represented in *Figure 3.1*.

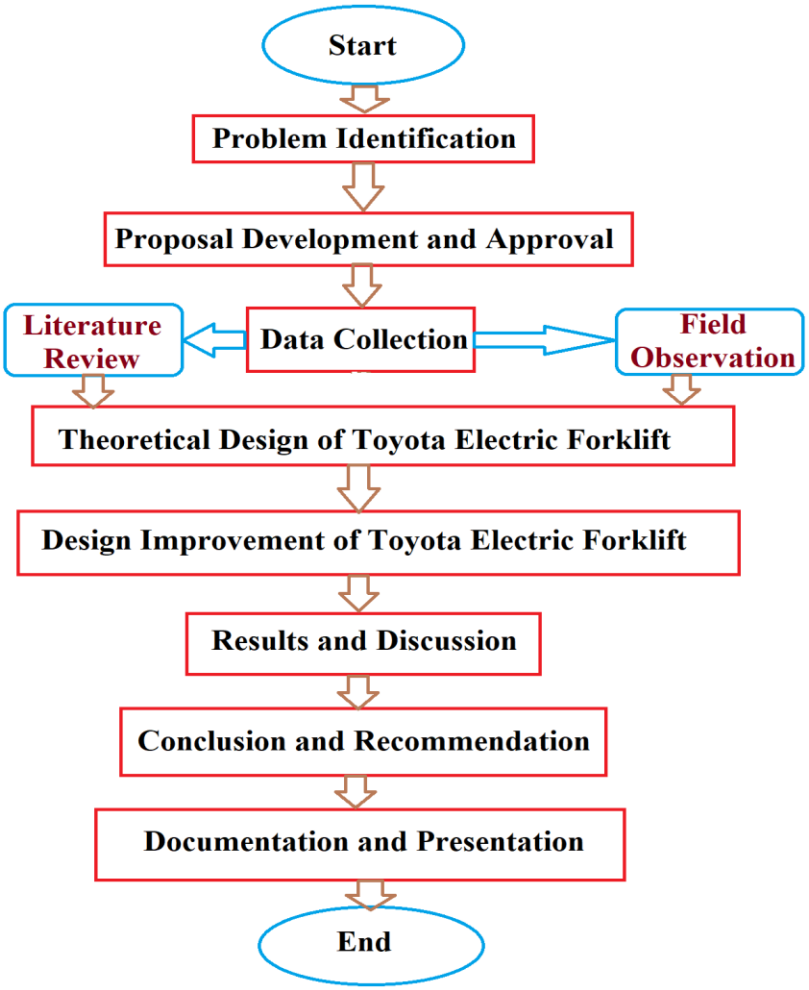

Figure 3.1: A Thesis flowchart

3.1. Research Design

This research will utilize an exploratory research design, which is a preliminary investigation aimed at gaining a better understanding of a phenomenon, generating new insights, and identifying potential hypotheses or ideas. Given that the design and improvement of electric forklift components placement is relatively new, this research design is highly suitable and will provide valuable insights into the study area.

The study aims to investigate two specific aspects: the external factors that make Toyota electric forklift parts vulnerable and the design vulnerabilities of these parts. The external factors to be examined may include environmental conditions like humidity, extreme temperatures and dust, among others. Additionally, the study will explore design vulnerabilities that contribute to the susceptibility of Toyota electric forklift parts, such as poor component layout, and improper mounting locations. Addressing these vulnerabilities is crucial as they can lead to increased maintenance costs, production downtime, and potential safety hazards.

3.2. Data Collection

In this thesis, a mixed-method approach will be employed to collect data. The approach consists of two main methods: document review, and visual observation.

3.2.1. Document review

A comprehensive review of relevant literature and documents related to electric forklifts is conducted. This will encompass studying literature on electric forklift components, maintenance practices, and external factors that can impact their performance. In addition, the part catalogue and repair manual of Toyota electric forklift 8FBMT40 model is consulted. Moreover, the official Toyota electric forklift website is visited to investigate the latest electric forklift design. The aim is to gather insights from existing information to inform the research.

3.2.2. Observation

In order to investigate the vulnerability of Toyota electric forklift to external factors visual observation is also performed. The observation is guided with two objectives. The first objective is to investigate the real-world experience of operating Toyota electric forklift. Whereas, the second objective is to identify the components and their placements that are vulnerable to external factors. In addition, determining the external factors which may cause the damage to these components is part of the observation.

3.3. Data Analysis

The results of the data collection are basically two things. These are, the components that are vulnerable to external factors, and the external factors that cause the damage to the components of the Toyota electric forklift. Hence, these two results are recorded and analyzed accordingly. Since it may be difficult to redesign all the components and their placement at once, priority is given to few components based on the downtime, operating and maintenance cost, the expense of redesign, and so on.

3.4. Design Improvements

After determining Toyota electric forklift design that are most vulnerable to failure and establish their root causes, the design improvements that could enhance the durability and reliability of the forklift parts are performed. One aspect of the design improvements will be a thorough analysis of the external factors that impact the performance of the electric forklift parts and components. The focus of these solutions is to reduce the vulnerability of the Toyota electric forklift parts and enhance their durability and reliability. The design improvements that considered here is better placement of parts to protect them from external elements that cause damage, and more accessible mounting locations for easy maintenance and repair.

3.5. CAD Modeling and Analysis

After the size and shape of the model are obtained through calculation, the new model is tested and compared with the previous model. The testing may include the availability test, the accessibility test, stress analysis, thermal analysis, and vibration test. Due to these, the geometry of the model is created using 3D software called SolidWorks. SolidWorks is a widely-used Computer-Aided Design (CAD) software that is employed by millions of engineers worldwide (Solidworks, 2022). It is equipped with a comprehensive set of features and tools, enabling users to create drawings, perform design analysis, estimate costs, generate renderings, and create animations, among other functions (Capitol Technology University, 2019). Additionally, it facilitates analyses and simulations, including Finite Element Analysis (FEA) (Solidworks, 2022). Renowned for its user-friendly interface, extensive functionality, and broad range of capabilities, it has become a favored choice for engineers and designers across diverse industries and professions worldwide (Capitol Technology University, 2019).

In addition, stress analysis, thermal analysis and vibration analysis is performed using ANSYS workbench software. ANSYS (Analysis System) is a leading engineering simulation software that offers a range of products for structural, fluid, and multiphysics analysis, including ANSYS Mechanical, which is a finite element solver with structural, thermal, acoustics, transient, and nonlinear capabilities, and ANSYS Fluent, which is known for fluid simulation. The software offers a dynamic environment with a complete range of analysis tools, from preparing geometry for analysis to connecting additional physics for even greater fidelity (ANSYS, 2021). Overall, it is a powerful and versatile software that can be used for a range of engineering simulation and 3D design applications (Huang & Dao, 2016).

Chapter Four

4. Design Improvements of Toyota Electric Forklift

4.1. Overview of the 8FBM 40 Toyota Electric Forklift

The Toyota 8FBM 40 electric forklift is a highly efficient and powerful machine specifically designed for indoor use within warehouses and manufacturing facilities. Toyota, a renowned brand in the forklift industry, has created one of their most popular models with the 8FBM 40. With a remarkable maximum capacity of 40,000 Kg and the ability to lift materials up to a height of 221 inches. The Toyota electric forklift 8FBM 40 proves to be an excellent choice for various purposes, including warehouse operations, storage facilities, and manufacturing plants. The model was first introduced in 2008 and has since become a popular choice for many businesses (Toyota Material Handling, 2023a).

Figure 4.1: 8FBM 40 Toyota electric forklift (Conger, 2023b)

The Toyota Electric Forklift 8FBM 40 has compact design that enables it effortless movement within tight spaces. In addition, it consists of the advanced AC drive system that ensures smooth acceleration and deceleration, enhancing efficiency. Moreover, it is equipped with a powerful electric motor, specifically a 48-volt AC electric motor, ensuring remarkable

performance and efficiency. Notably, it incorporates regenerative braking, enhancing battery life and minimizing energy usage. It can handle a variety of loads, including pallets, boxes, and containers. The forklift features a low center of gravity that helps to reduce the risk of tipping over (Conger, 2023b).

The Toyota 8FBM 40 electric forklift offers several advantages over internal combustion models, including lower operating costs and environmental friendliness with zero emissions (Toyota Material Handling, 2023a). Its versatility and efficiency are also notable due to its electric motor, providing excellent performance while consuming minimal energy (Gaines et al., 2008). However, electric forklifts may not be suitable for all applications, such as outdoor use or heavy lifting, where internal combustion forklifts may be a better option. Additionally, the need for a charging station can be a costly installation requirement. While electric forklifts generally require low maintenance, the 8FBM 40 may require specialized parts and technicians for repairs due to its advanced technology (Conger, 2023b).

In the current design of the 8FBM 40 Toyota Electric Forklift the components are arranged in such a way as to ensure that the operator has an unobstructed view of the lifting area. The forklift's control panel, including the steering wheel and drive joystick, is conveniently located to the left of the operator's seat. The batteries, which power the electric motor, are located under the operator's seat for optimal weight distribution and easy maintenance. According to (Toyota, 2023), the layout of the 8FBM 40 forklift is intended to maximize the efficiency and safety of the operator.

However, the layout of the components in the 8FBM 40 forklift may pose some maintenance challenges. Because the batteries are located under the operator's seat, routine maintenance tasks such as battery replacement or fluid level checks require additional time and effort to access the battery compartment. Additionally, this location may increase the risk of contamination from dirt or water, which could compromise the batteries' performance. To mitigate this, Toyota recommends regular cleaning of the battery compartment and careful attention to the recommended operating and maintenance procedures.

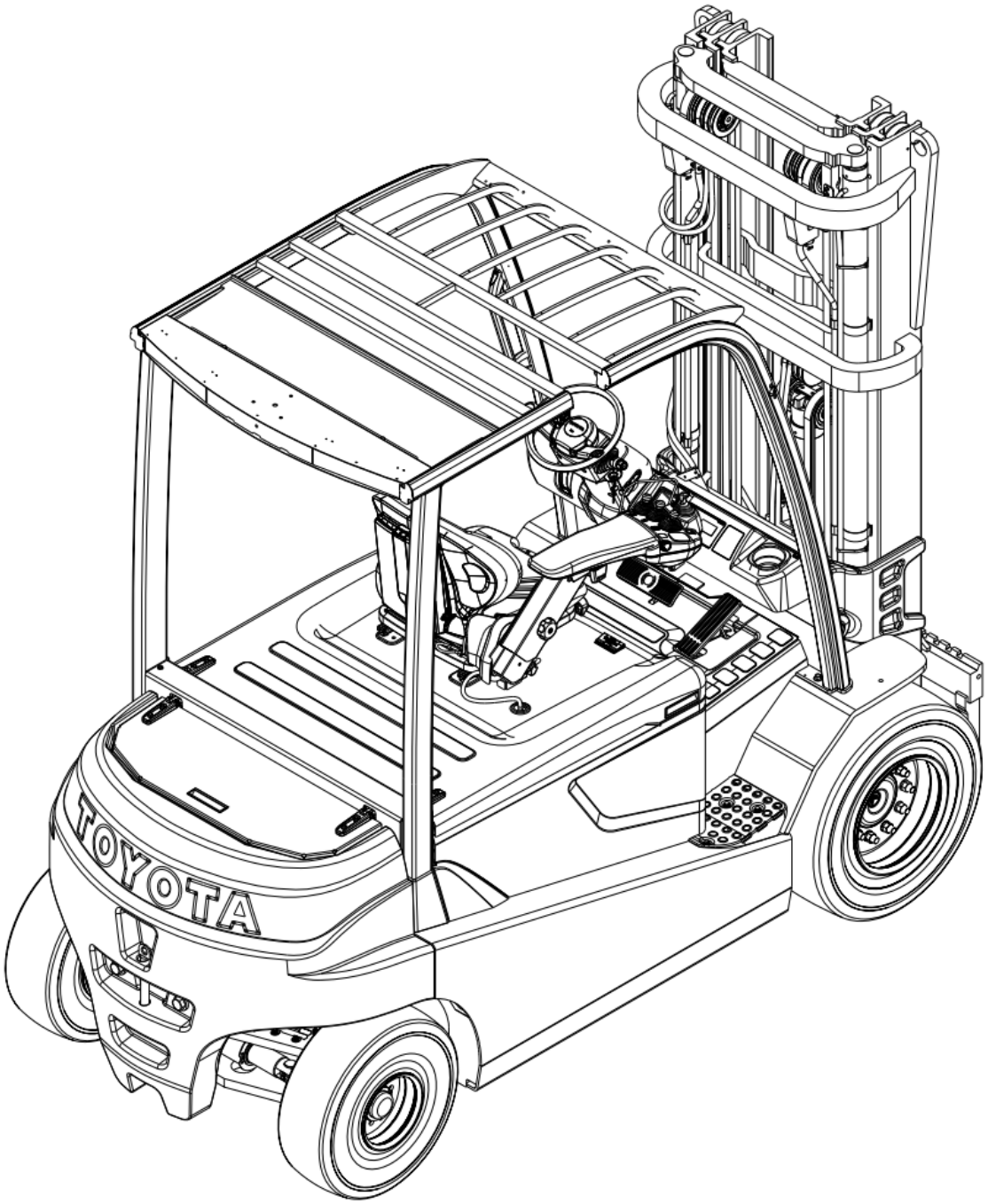

Figure 4.2: 8FBM 40 Toyota Electric Forklift (Toyota Material Handling Company, 2015)

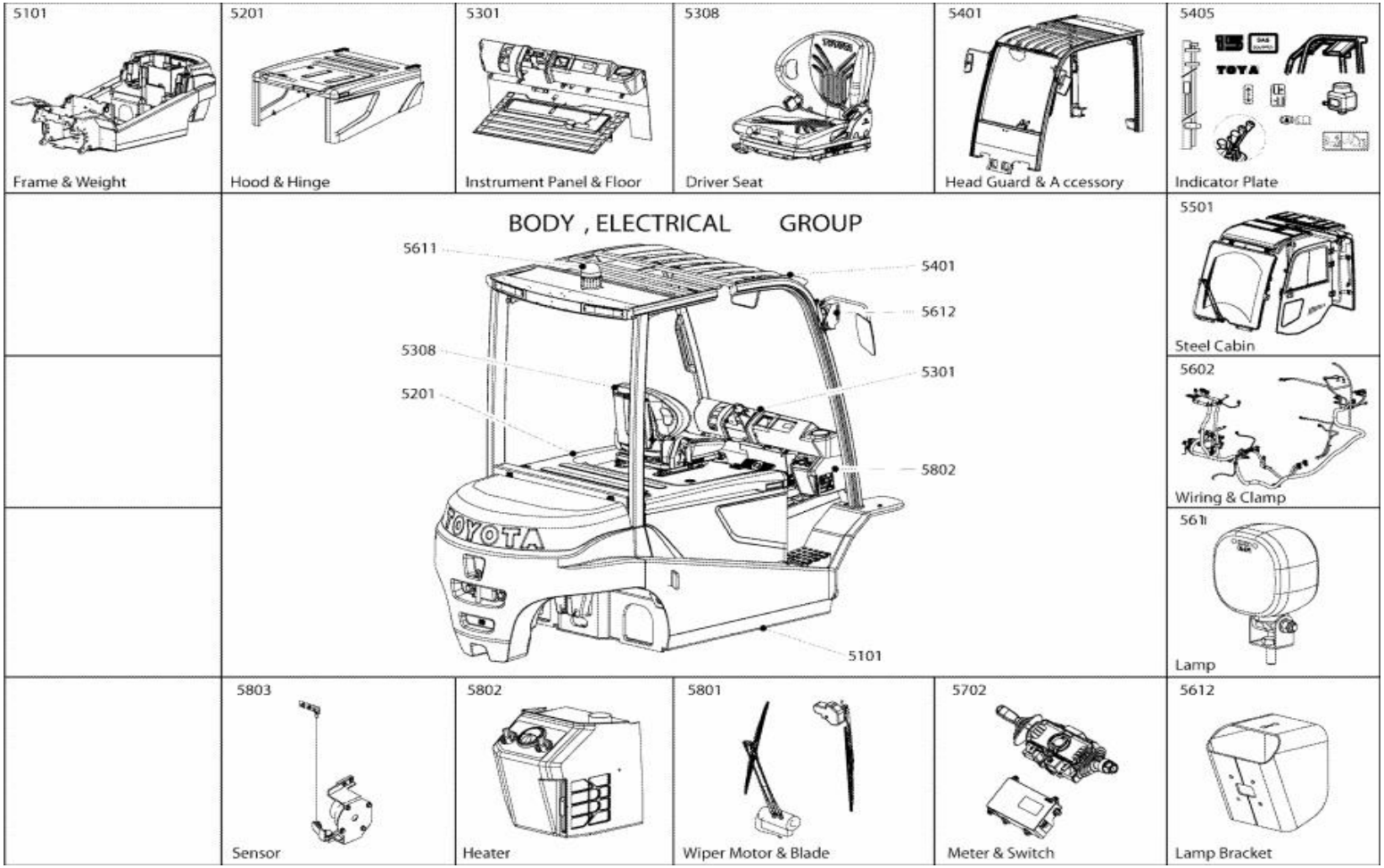

Figure 4.3: Detail drawing of 8FBM 40 Toyota Electric Forklift body and electrical group (Toyota Material Handling Company, 2015)

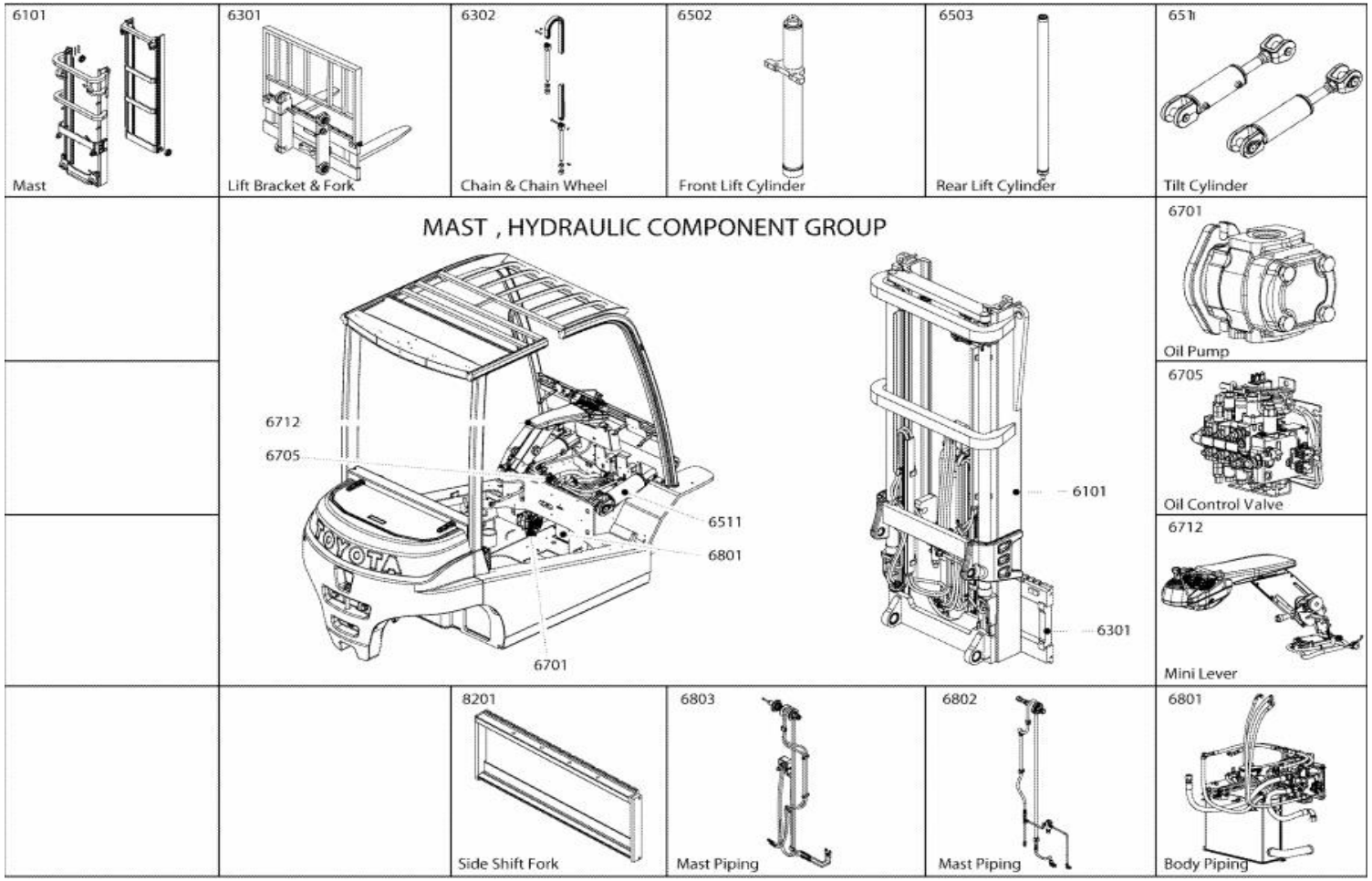

Figure 4.4: Detail drawing of 8FBM 40 Toyota Electric Forklift mast and hydraulic group (Toyota Material Handling Company, 2015)

Table 4.1: various basic components of 8FBM 40 Toyota Electric Forklift and their respective weight (Toyota Material Handling Company, 2015)

S.No.	Components	Weight (Kg)
1	Battery	2069 – 2287
2	Front axle assembly	480
3	Pump motor unit	63
4	Rear axle assembly	217
5	Counterweight	561
6	Rear chassis	695
7	Mast assembly (excluding the fork)	475
Total		4,560 – 4,778

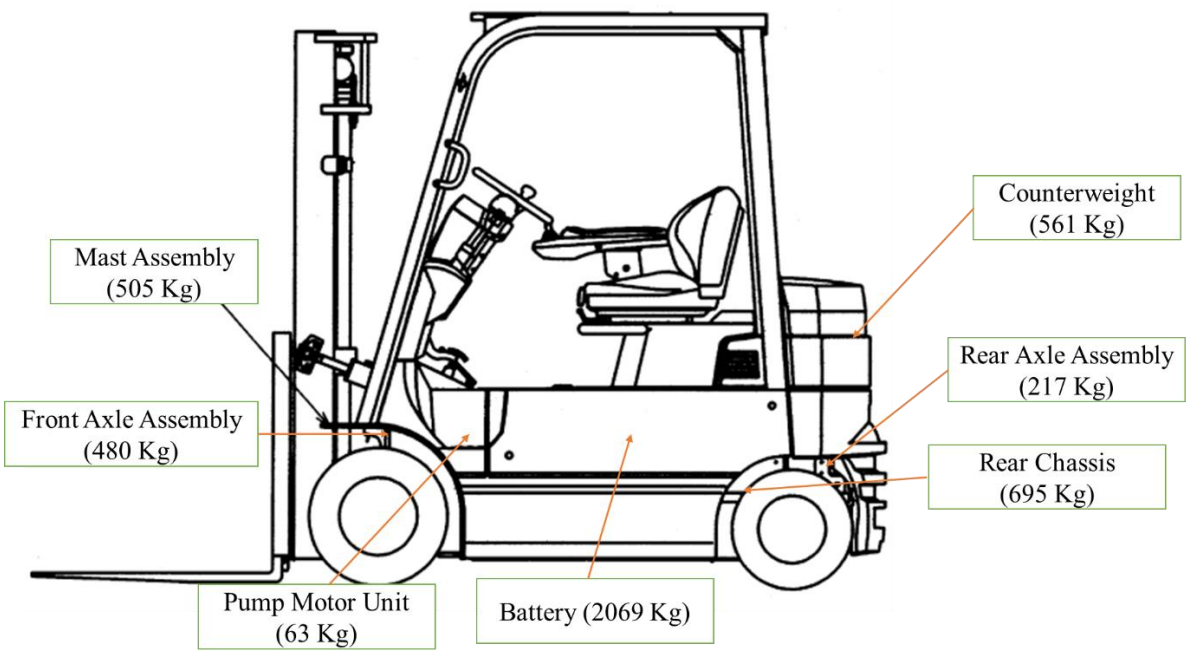

Figure 4.5: various basic components of 8FBM 40 Toyota Electric Forklift and their respective weight (Toyota Material Handling Company, 2015)

Moreover, components such as pump motor and oil pump are only accessible after battery is removed from its compartment as shown in *Figure 4.6* and, *Table 4.4* and *Table 4.5*. This is very difficult due to two reasons. The first reason is that the battery weighs about two tonnes

as shown in *Table 4.1*, and it is difficult to remove the battery every time the maintenance is required for the pump motor or oil pump. The second reason is that it is very difficult for single operator to do maintenance alone.

Table 4.2: Oil Pump Specification for 8FBM 40 Toyota Electric Forklift (Toyota Material Handling Company, 2015)

Oil Pump type	PHP20.24,5S0-07WL-LGF/OD-N-QW
Oil Pump name	Gear Pump
Engine System	direct motor activation
Nominal leakage (cm^3/rev)	25.305

In addition, the battery cannot be removed by bare hand other lifting mechanisms are required. And, this increases the downtime of the machine, increase the cost of operation and reduce the efficiency of the system.

Table 4.3: Pump motor Specification for 8FBM 40 Toyota Electric Forklift (Toyota Material Handling Company, 2015)

Voltage	53 Vac
Current	381A
Power	25.5 KW
Speed	2280 rpm
Efficiency	85.7
Type of connection	Δ
Degree of protection (Ip code)	IP 20

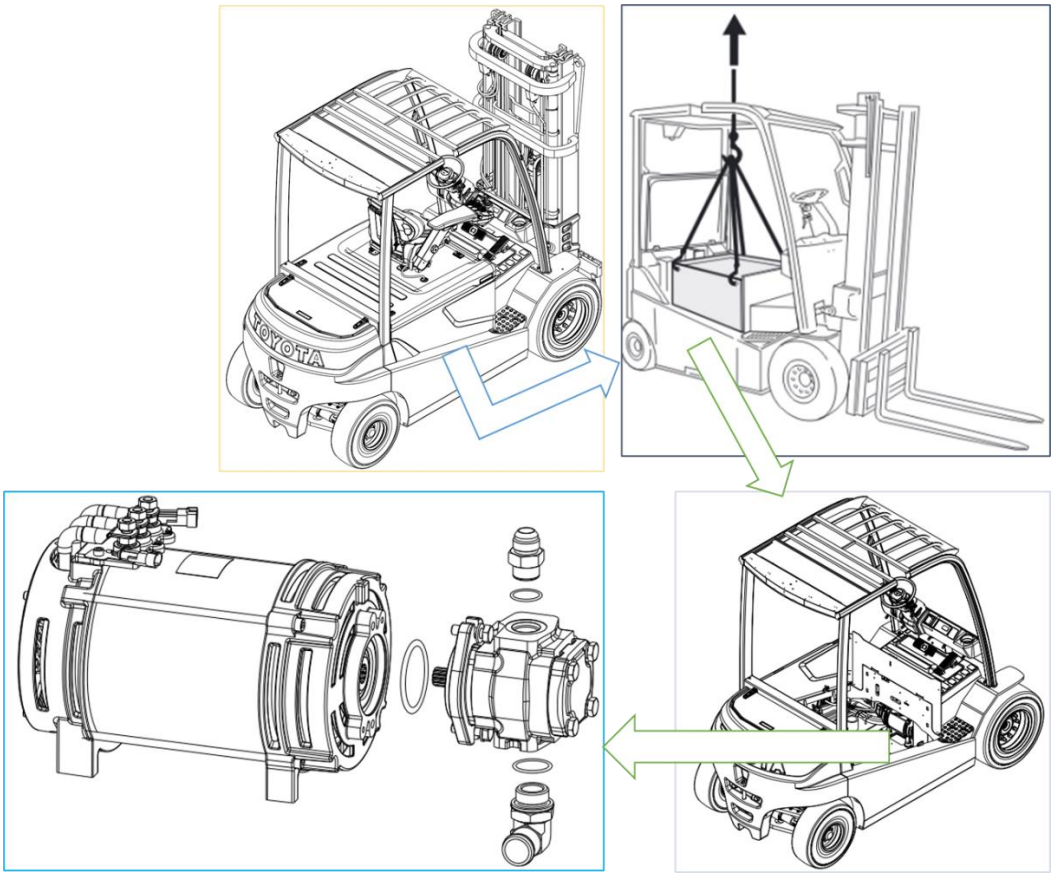

Figure 4.6: Pump motor of 8FBM 40 Toyota Electric Forklift disassembly procedure (Toyota Material Handling Company, 2015)

Furthermore, in addition to the unavailability for maintenance, the current placement of pump motor and oil pump of 8FBM 40 Toyota Electric Forklift makes them vulnerable to dirt and water. This is due to two reasons. The components are only few centimeters from the floor and the protective device are not installed for them.

Table 4.4: Disassembly procedure for pump motor 8FBM 40 Toyota Electric Forklift (Toyota Material Handling Company, 2015)

Step	Procedures
1	Turn the rear mast sideways and lower the forks to the ground.
2	Remove the battery
3	Empty the hydraulic oil tank
4	Disconnect the hoses from the pump
5	Remove the two pump fixing screws.
6	Remove the hydraulic pump.
7	Disconnect the power cables and the wiring from the pump motor.
8	Unscrew the fixing nuts and remove the pump motor.

Table 4.5: Disassembly procedure for oil pump 8FBM 40 Toyota Electric Forklift (Toyota Material Handling Company, 2015)

Step	Procedures
1	Turn the rear mast sideways and lower the forks to the ground.
2	Remove the battery
3	Empty the hydraulic oil tank
4	Disconnect the hoses from the pump
5	Remove the two pump fixing screws.
6	Remove the hydraulic pump.
7	Remove the connections from the pump

Hence, for the ease of maintenance and avoiding vulnerability to external factors, 8FBM 40 Toyota Electric Forklift components placement need to be improved. Components those to be relocate to the new location are hydraulic oil pump with pump motor and hydraulic oil tank. Moreover, during the maintenance of both hydraulic oil pump and pump motor, the maintenance procedure suggested that the hydraulic oil tank to be empty. This increase the operation cost and moreover, increase the impact of the machine on the environment. But this can be mitigated with the help of oil cooler. However, the current design of 8FBM 40 Toyota

Electric Forklift do not have the oil cooler. Therefore, in addition to relocating the pump motor and oil pump of 8FBM 40 Toyota Electric Forklift, it is necessary to incorporate oil cooler to the new design.

Electric forklifts require less maintenance than internal combustion forklifts due to having fewer moving parts. However, they still require regular maintenance to operate at maximum efficiency and lifespan. The batteries and other electrical components require regular care, including watering the battery regularly, monthly cleaning, equalizing, regular technician checks, use of proper charging techniques and equipment, and blowing out the forklift regularly. Loose motor cables can interfere with the operation of the forklift and cause damage or even contribute to a fire. Conducting comprehensive maintenance on the forklift, including daily checks of all elements, can help extend the life of the machine and prevent major accidents and downtime (darrequipment, 2019).

There are various possible design improvements that can be implemented to reduce the vulnerability of Toyota electric forklift to external factors. One of such design improvement is the relocation of vulnerable components. For the ease of maintenance and avoiding vulnerability to external factors, 8FBM 40 Toyota Electric Forklift components placement need to be improved. However, there are various factors that need to be considered to determine the optimum design of the new location. These are:

- Accessibility of the new location,
- Space availability,
- Weight distribution,
- Vibration generated, and
- Heat dissipation and cooling requirement.

Accessibility for maintenance is an important criterion when relocating a component. The new location should be easily accessible for maintenance and repairs, as well as for routine checks by the operator, such as checking oil levels. Accessibility of the machine part for maintenance can be affected by:

- The size and shape of the component,
- The proximity of other components,
- The presence of obstructions, such as pipes or cables, and
- The clearance required for maintenance activities.

In addition, when relocating the component of a Toyota electric forklift, it is important to evaluate the available space on the forklift. This involves considering potential interference with other components or structures and ensuring there is enough room for the component to operate safely. The new location should have enough space to accommodate the component and its accessories.

Moreover, the new location should not affect the weight distribution of the forklift. This can impact the stability, maneuverability and safety of the forklift. To calculate weight distribution for an electric forklift, there are a few factors that need to be taken into consideration. These include:

- The weight of the forklift itself,
- The weight of the load being carried,
- The position of the load on the forklift, and
- The center of gravity of the forklift and load.

Additionally, the pump motor generates heat and vibration during operation. Therefore, it is required to ensure that the new location provides adequate ventilation and cooling to prevent overheating and potential damage to the motor. The pump motor also requires cooling, so the new location must have adequate airflow. Moreover, the pump motor vibrates during operation, so the new location should be isolated from other components that are sensitive to vibration. And, it should be considered that the motor is positioned away from any potential hazards or areas prone to damage, and the new location should allow for proper routing of cables and connections, minimizing any potential for damage or interference.

4.2. Relocating hydraulic oil pump with pump motor

The pump motor and oil pump are important components 8FBM 40 Toyota Electric Forklift. The pump motor and oil pump work together to ensure that the hydraulic system has the necessary oil flow to operate properly. The pump motor provides the power to drive the oil pump, and the oil pump delivers the oil to the various components of the system. 8FBM 40 Toyota Electric Forklift uses gear pump.

Gear pumps are a type of positive displacement (PD) pump used to move fluids by enclosing a fixed volume using interlocking gears (michael-smith-engineers, 2020). They operate at speeds between 1,700 and 4,500 rpm for small models and below 1,000 rpm for larger models. Gear pumps work by carrying fluid between the teeth of two meshing gears, creating a partial vacuum at the suction and forcing the fluid out at the discharge (Almasi, 2017).

Gear pumps can be of two basic designs: external and internal. External gear pumps consist of two identical, interlocking gears supported by separate shafts, while internal gear pumps have two interlocking gears of different sizes with one rotating inside the other. They are compact and simple with a limited number of moving parts, making them particularly suited for pumping oils and other high viscosity fluids. They are self-priming and can dry-lift, although their priming characteristics improve if the gears are wetted (michael-smith-engineers, 2020).

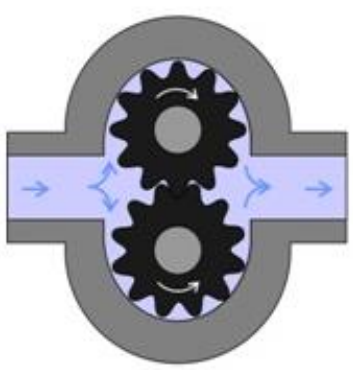

External Gear Pump

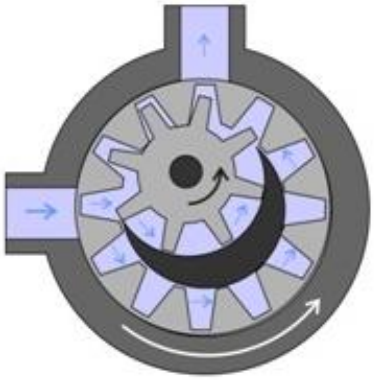

Internal Gear Pump

Figure 4.7: Gear pump designs (michael-smith-engineers, 2020)

External gear pumps are capable of sustaining higher pressures and flow rates because of the more rigid shaft support and closer tolerances, making them well-suited for high-pressure applications. They are often used for pumping water, light oils, chemical additives, resins, or solvents. Internal gear pumps have better suction capabilities and are suited to high viscosity fluids (Almasi, 2017).

In the current design of 8FBM 40 Toyota Electric Forklift, pump motor is only accessible after battery is removed from its compartment as shown in *Figure 4.6*. This is very difficult since the battery weighs about two tonnes, and it is difficult to remove the battery every time the maintenance is required for the pump motor. Thus, it is necessary to relocate the pump motor by considering various factors discussed above. As such, three possible locations are identified for further analysis, as shown in *Figure 4.8*. These possible locations are: the right side of the forklift, the left side of the forklift, and the rear side of the forklift.

Accessibility for maintenance is one of the criteria for determining the optimum location for pump motor relocation. If the pump motor is not accessible, it may be difficult or impossible to perform necessary repairs or maintenance, which could lead to premature failure of the pump motor.

Table 4.6: Dimensions of pump motor and oil pump

S.No.	Parameter	Value
1	Motor outside diameter (mm)	180
2	Motor overall length (mm)	330
3	Pump outside diameter (mm)	120
4	Pump overall length (mm)	160

Pump motor assembly with oil pump can be considered as the cylinder with the diameter of 180 mm and length of 490 mm, as shown in *Table 4.6*. From the options discussed above,

option 1 and option 1 have available space of: width = 116 mm and length = 1028 mm, as shown in *Figure 4.9* and *Appendix 1*. Whereas, width = 1113 mm and length = 462.5 mm, as shown in *Figure 4.9* and *Appendix 1*.

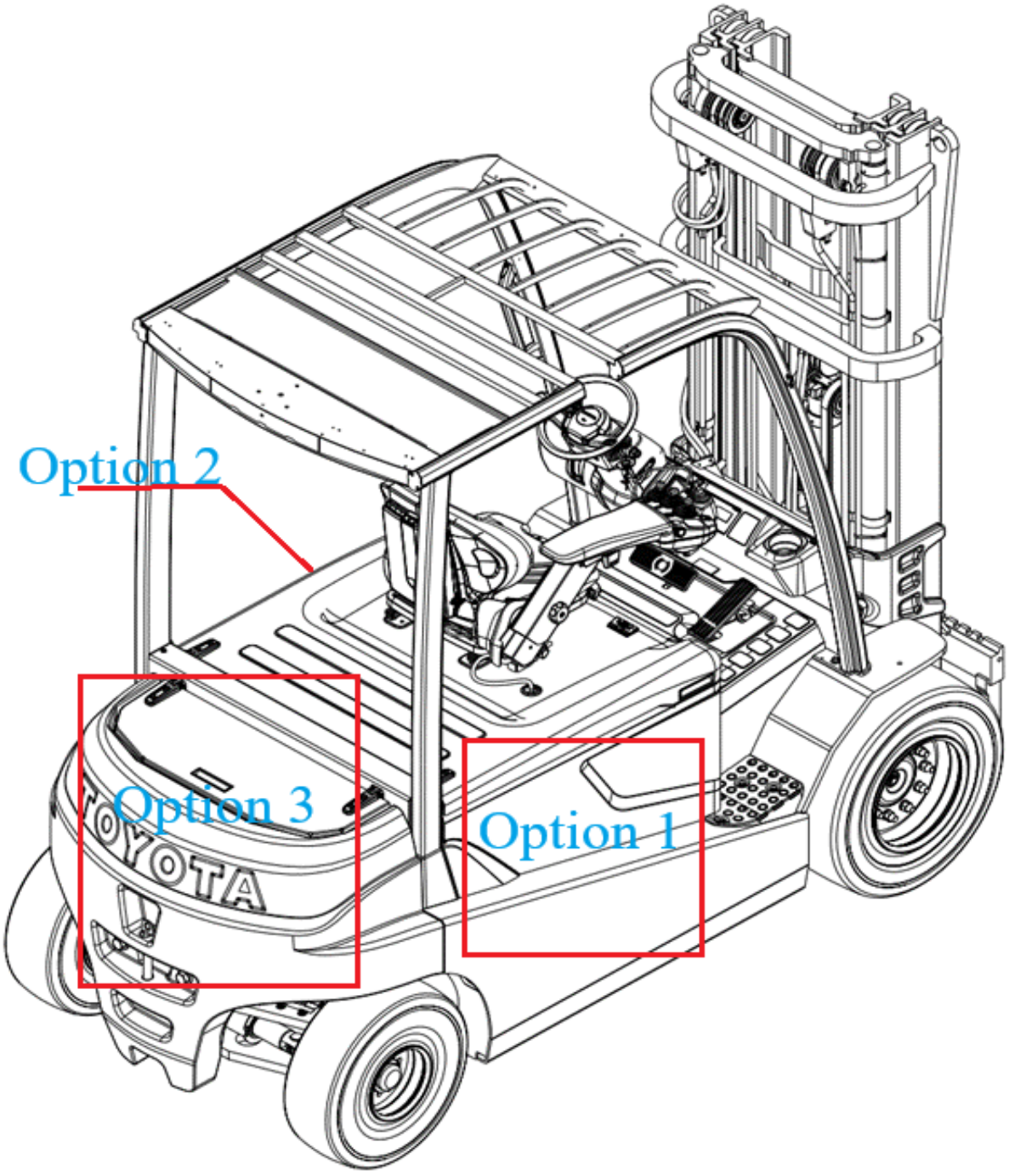

Figure 4.8: Possible new location for relocation of the components

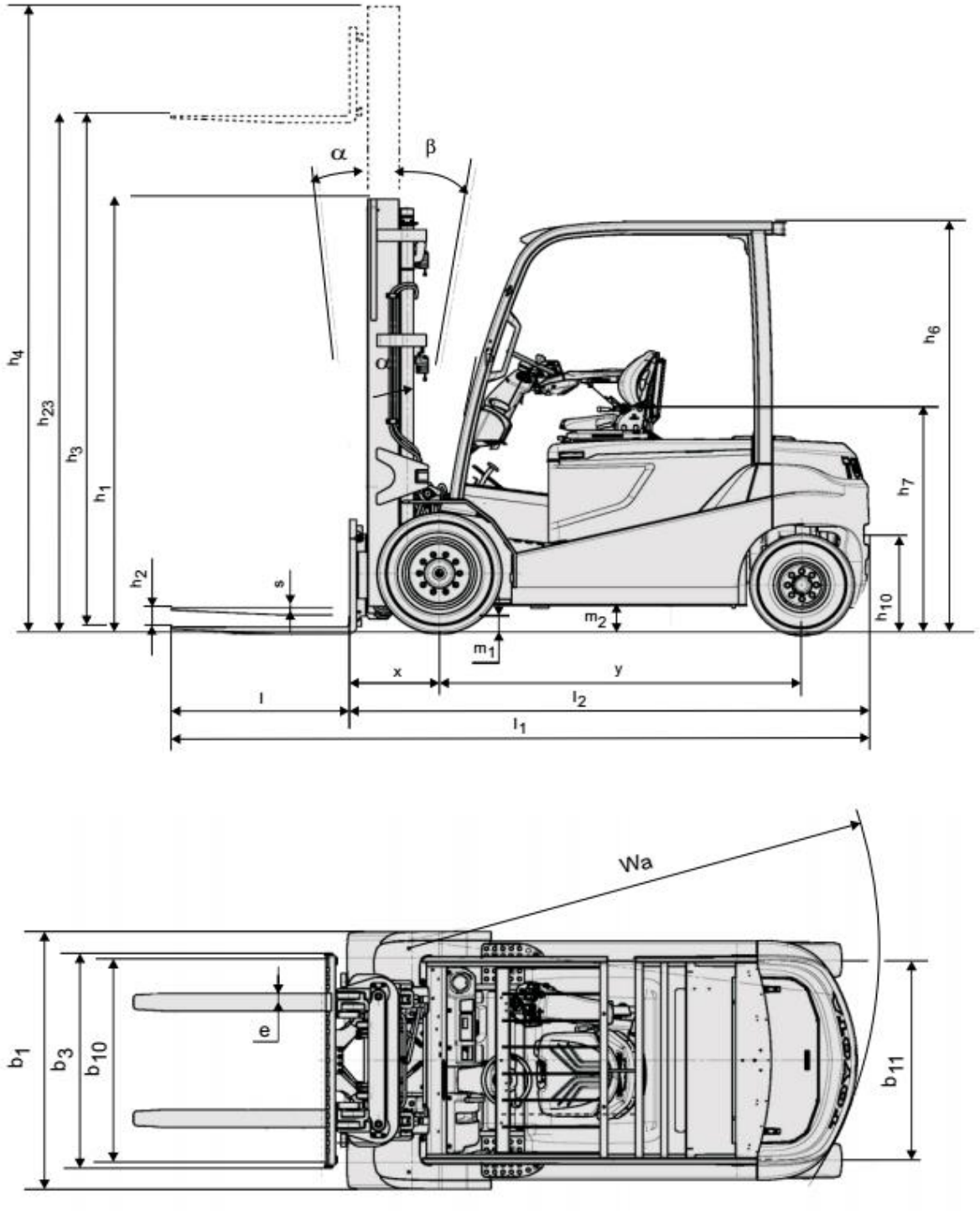

Figure 4.9: Dimensional drawings of 8FBM40 Toyota Electric Forklift (Toyota Material Handling, 2023b)

By rearranging the width and length of option 3:

Table 4.7: Available space for relocation

Parameter	Required space for relocation	Option 1	Option 2	Option 3
Width (mm)	180	116	116	462.5
Length (mm)	490	1028	1028	1113

For Option 1:

$$w_{a1} = 116\ mm \text{ and } L_{a1} = 1028\ mm$$

$$w_r = 180\ mm \text{ and } L_r = 490\ mm$$

$$w_{a1} < w_r$$

$$L_{a1} > L_r$$

With rearranging the width and length,

$$L_{a1} = 116\ mm \text{ and } w_{a1} = 1028\ mm$$

$$w_r = 180\ mm \text{ and } L_r = 490\ mm$$

$$w_{a1} > w_r$$

$$L_{a1} < L_r$$

That is, the available width from option 1 is less than that of the space required. Whereas, the available length from option 1 is greater than that of the space required. That is, the available space is not enough to accommodate the component. Even with rearranging the width and length, the available space is not enough to accommodate the component.

For Option 2:

$$w_{a2} = 116\ mm \text{ and } L_{a2} = 1028\ mm$$

$$w_r = 180\ mm \text{ and } L_r = 490\ mm$$

$$w_{a2} < w_r$$

$$L_{a2} > L_r$$

With rearranging the width and length,

$$L_{a2} = 116\ mm \text{ and } w_{a2} = 1028\ mm$$

$$w_r = 180\ mm \text{ and } L_r = 490\ mm$$

$$w_{a2} > w_r$$

$$L_{a2} < L_r$$

That is, the available width from option 2 is less than that of the space required. Whereas, the available length from option 2 is greater than that of the space required. That is, the available space is not enough to accommodate the component. Even with rearranging the width and length, the available space is not enough to accommodate the component.

For Option 3:

$$w_{a3} = 462.5\ mm \text{ and } L_{a3} = 1113\ mm$$

$$w_r = 180\ mm \text{ and } L_r = 490\ mm$$

$$w_{a3} > w_r$$

$$L_{a3} > L_r$$

That is, the available width from option 3 is greater than that of the space required. Moreover, the available length from option 3 is greater than that of the space required. That is, the available space is enough to accommodate the component.

Thus, option 3 has more space to accommodate the pump motor with oil pump than that of option 1 and option 2.

Therefore, the total volume of the assembly can be calculated from:

$$V_C = \frac{\pi d^2 h}{4}$$ Equation 4-1

Where:

- V_C is the volume of the component,
- d is the overall diameter of the assembly, and
- h is the overall length of the assembly.

Thus,

$$V_C = \frac{3.14 * 0.18^2 * 0.49}{4}$$

$$\mathbf{V_C = 0.01246\ m^3}$$

Whereas the total available volume for accommodation can be determined from:

$$V_t = w * L * h$$ Equation 4-2

Where:

- V_t is the total available volume for the component to occupy,
- w is the available width,
- L is the available Length, and
- h is the available height.

Thus, with the dimensions from *Table 4.7* and *Appendix 1*

$$V_t = 0.4625 * 1.113 * 0.727$$

$$\mathbf{V_t = 0.3742\ m^3}$$

The accessible volume is calculated by:

$$V_a = V_t - V_C$$ Equation 4-3

Where:

- V_a is accessible volume which is the volume of the space around the component that is accessible for maintenance,
- V_t is the total volume of the space occupied by the component, and
- V_C is the volume of the component.

$$\mathrm{V_a} = 0.3742 - 0.01246$$

$$\mathbf{V_a = 0.36174\ m^3}$$

Accessibility for maintenance can be determined by:

$$A_S = \frac{V_a}{V_t} * 100 \qquad \text{Equation 4-4}$$

Where:

- A_S is accessibility score for maintenance of the component,
- V_a is accessible volume which is the volume of the space around the component that is accessible for maintenance, and
- V_t is the total volume of the space occupied by the component.

$$A_S = \frac{0.36174}{0.3742} * 100$$

$$\mathbf{A_S = 96.67\%}$$

Thus, by considering option 3, it is possible to obtain 96.67% of the accessibility score. This indicates, the components are accessible directly from this location.

The next factor to consider is the weight distribution of the forklift. The new location should not affect the weight distribution of the forklift. This can impact the stability and safety of the forklift. And one way to calculate weight distribution is to use the load center. The load center is the horizontal distance between the load's center of gravity and the front face of the forks. To calculate weight distribution, the load center should be multiplied by the weight of the load. This will give the weight moment, which is the force that is applied to the forklift's center of gravity.

$$w_d = \frac{d_{ax}}{b_w} w_L$$ Equation 4-5

Where:

- w_d is the weight distribution,
- d_{ax} is the distance from front axle to load center,
- b_w is the wheel base, and
- w_L is the load weight.

Here, the distance from the front axle to the load center is the horizontal distance between the load's center of gravity and the front axle of the forklift. The wheelbase is the distance between the front and rear axles of the forklift.

Alternatively,

$$w_d = \frac{W_f d_f}{(d_f + d_r)}$$ Equation 4-6

Where:

- w_d is the weight distribution on the front axle,
- w_f is the forklift weight,
- d_f is the front axle position, and
- d_r is the rear axle position.

Here, forklift weight is the weight of the forklift without any load, front axle position is the distance from the front of the forklift to the front axle, and rear axle position is the distance from the front of the forklift to the rear axle.

According to *Table 4.1* and *Appendix 1*, the total weight of the forklift without load is 4560 Kg, the weight of the pump unit is 63 Kg, the weight of the counterweight is 561, the front axle position is 518 mm, and the rear axle position is 2548. Thus, the weight distribution of the old system can be determined from *Equation 4-6* as follows:

$$w_d = \frac{4560 * 0.518}{(0.518 + 2.548)}$$

$$\mathbf{w_d = 770.411\ Kg}$$

That is, from 4560 of the total forklift weight 770.411 Kg weight is on the front axle. Whereas, the remaining 3,789.589 Kg weight is on the rear axle.

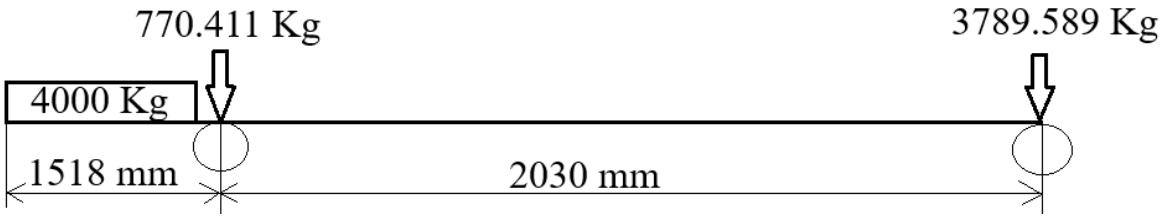

Figure 4.10: Weight distribution of the current design

Hence, the relocation of the components should follow such arrangement. This could be done in three steps. These are:

- Step 1: Removing the pump motor unit from the front axle:

With the current installation or arrangement, pump motor is on the front axle, as shown in *Figure 4.5*. Thus, to relocate the pump motor unit, it is required to remove the unit from this place. Thus, without the pump motor unit, the weight on the front axle will be:

$$W_{nf} = W_{of} - W_{pm} \qquad \text{Equation 4-7}$$

Where:

- W_{nf} is the weight on the front axle after pump motor unit is removed,
- W_{of} is the weight on the front axle before pump motor unit is removed, and
- W_{pm} is the weight of the pump motor unit.

$$W_{nf} = 770.411 - 63$$

$$\mathbf{W_{nf} = 707.411\ Kg}$$

Thus, after the pump motor unit is removed, the weight on the front axle become 707.411 Kg.

- Step 2: Counterbalancing the weight removed from front axle:

Since the pump motor is removed from the front axle, it is required to counterbalance the weight. This can be done in two ways. The first one is to replace the same weight as that of removed weight in the pump motor unit place. The second one is removing the same amount of weight from the rear axle. This means removing the weight from the counterweight. Since the pump motor unit is going to be in this place and reducing the weight is more economical than adding the weight, the second option is more feasible. Thus, without the pump motor unit, the weight on the front axle is 707.411 Kg. Thus, 63 Kg of weight is needed to be removed from the rear axle to counterbalance the weight of the pump motor unit removed from the front axle. Thus, the weight on the rear axle will be:

$$W_{nr} = W_{or} - W_{pm} \qquad \text{Equation 4-8}$$

Where:

- W_{nr} is the weight on the rear axle after pump motor unit is removed from front axle,
- W_{or} is the weight on the rear axle before pump motor unit is removed, and
- W_{pm} is the weight of the pump motor unit.

$$W_{nr} = 3{,}789.589 - 63$$

$$\mathbf{W_{nr} = 3{,}726.589\ Kg}$$

Thus, after the pump motor unit is removed from the front axle, the weight on the rear axle become 3,726.589 Kg.

- Step 3: Relocating the pump motor unit

As indicated on *Figure 4.8*, and discussed above, the viable option for relocating the pump motor unit is option 3. However, option 3 puts the load on the rear axle. Therefore, to

relocate the pump motor unit without affecting the stability of the forklift, we need to remove similar weight as that of pump motor unit. Thus, since pump motor unit weighs 63 Kg, 63 kg of mass should be removed from the rear axle. Thus, the weight on the rear axle will be:

$$W_{nr1} = W_{nr} - W_{pm} \qquad \text{Equation 4-9}$$

Where:

- W_{nr1} is the weight on the rear axle after removing weight for relocating pump motor unit,
- W_{nr} is the weight on the rear axle after pump motor unit is removed from front axle, and
- W_{pm} is the weight pump motor unit.

$$W_{nr1} = 3{,}726.589 - 63$$

$$\mathbf{W_{nr1} = 3{,}663.589\ Kg}$$

Thus, after the pump motor unit is removed from the front axle, the weight on the rear axle become 3,663.589 Kg.

Therefore, without affecting the stability of the forklift, 126 Kg of weight is needed to be removed from the rear axle, without affecting the functionality of the components, as shown in *Figure 4.11*. However, there are four basic assemblies which their weight affect the load on the rear axle, as shown in *Figure 4.5*. These are battery pack, rear axle assembly, rear chassis and counterweight. This is from those assemblies and components, the only possible way to remove weight is from the counterweight. Currently, counterweight has a weight of 561 Kg. Thus, the new weight of the counterweight, W_{ncw} can be determined from:

$$W_{ncw} = 561 - 126$$

$$\mathbf{W_{ncw} = 435\ Kg}$$

Therefore, after relocating the pump motor unit, the new counterweight of the forklift weighs only 435 Kg.

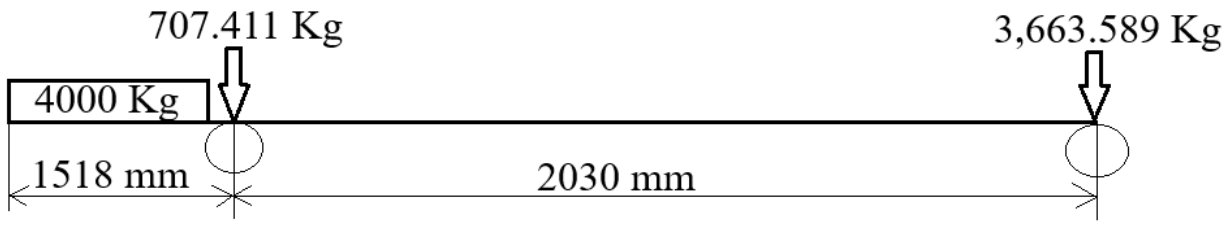

Figure 4.11: Weight distribution of the new design after pump motor relocation

Then, the next factor to consider is the heat dissipation requirement of the pump motor. The heat dissipation requirements of the pump motor for an electric forklift can be calculated using the following formula:

$$Q_D = P_{pm}(1 - \eta_{pm}) \qquad \text{Equation 4-10}$$

Where:

- Q_D is the heat dissipation requirements, in w
- P_{pm} is the power consumption of the pump motor, in w, and
- η_{pm} is the efficiency of the pump motor.

Power consumption of the pump motor is the amount of electrical power that the pump motor consumes. And, efficiency of the pump motor is the percentage of the power consumed by the pump motor that is converted into useful work. The heat dissipation requirements can be increased by factors such as the ambient temperature, the load on the pump motor, and the type of lubricant used. It is important to ensure that the pump motor has adequate cooling in order to prevent overheating. Alternatively, the heat dissipation requirements of the pump motor for an electric forklift can be determined from:

$$Q_D = (P_m \eta_m) - (P_p \eta_p) \qquad \text{Equation 4-11}$$

Where:

- Q_D is the heat dissipation requirements, in w
- P_m is the power consumption of the motor, in w,

- η_m is the efficiency of the motor.
- P_p is the power consumption of the pump, in w, and
- η_p is the efficiency of the pump.

Therefore, using *Equation 4-10*, and from *Table 4.3*: $\mathrm{P_{pm}} = 25.5\ kW$ and $\eta_{\mathrm{pm}} = 0.857$.

$$\mathrm{Q_D} = \mathrm{P_{pm}}(1 - \eta_{\mathrm{pm}})$$

$$\mathrm{Q_D} = 25.5(1 - 0.857)$$

$$\mathbf{Q_D = 3.6465\ kW}$$

Thus, the heat dissipation of the pump motor is 3.6465 kW. Then, the temperature increase of the fluid in the pump, considering Azolla 32 as hydraulic fluid, *Table 4.8*, can be determined from:

$$\mathrm{Q_D} = \dot{\mathrm{m}}_{\mathrm{o}}\mathrm{Cp_o}\Delta T_{fp} = \rho_o \dot{V}_{\mathrm{o}}\mathrm{Cp_o}\Delta T_{fp} \qquad \text{Equation 4-12}$$

$$\Delta T_{fp} = \frac{\mathrm{Q_D}}{\rho_o \dot{V}_{\mathrm{o}}\mathrm{Cp_o}}$$

Where:

- Q_D is the heat dissipation requirements,
- $\dot{\mathrm{m}}_{\mathrm{o}}$ is the mass flow rate of the pump,
- ρ_o is the density of the hydraulic oil, 875 kg/m^3 from *Table 4.8*,
- $\dot{V}_{\mathrm{o}}$ is the maximum volume flow rate of the pump, 0.0015 m^3/s (Toyota Material Handling, 2023b),
- $\mathrm{Cp_o}$ is the specific heat of the hydraulic oil, 2.418 kJ/KgK from *Table 4.8*, and
- ΔT_{fp} is the temperature change in the pump.

$$\Delta T_{fp} = \frac{3.6465}{875 * 0.0015 * 2.418}$$

$$\mathbf{\Delta T_{fp} = 1.149\ ℃}$$

Therefore, the pump gain 1.149 ^{O}C temperature while dissipating 3.6465 kW of heat to the atmospheric air. Since this value is small, there is no risk of overheating.

Table 4.8: Properties of the hydraulic oil used in 8FBM40 Toyota Electric Forklift

S.No.	Property	Azolla 32	Rando HD 32
1	Density (Kg/m^3)	875	870
2	Kinematic viscosity (mm^2/s)	32	28.8
3	Dynamic viscosity (mPa-s)	0.0032	0.0068
4	Specific heat at constant pressure (KJ/KgK)	2.418	2.4
5	Thermal conductivity (w/mK)	0.14	0.12
6	Prandtl Number	145	350

In addition, the vibration generated by the pump motor should be considered before relocating it. The vibration generated by the pump motor of an electric forklift can be calculated as follows:

The angular frequency can be calculated as follows:

$$\alpha_f = \frac{2\pi rpm}{60} \qquad \text{Equation 4-13}$$

Where:

- α_f is the angular frequency which is the frequency of the vibration, measured in radians per second, and
- rpm is the rotational speed of the pump motor, measured in revolutions per minute, is 2280 rpm from *Table 4.3*.

That is:

$$\alpha_f = \frac{2\pi * 2280}{60}$$

$$\boldsymbol{\alpha_f = 238.76\ s^{-1}}$$

Then,

$$A = \sqrt{\frac{m\alpha_f^2 S}{m\alpha_f^2 + ב^2}}$$ Equation 4-14

Where:

- A is the vibration amplitude which is the measure of the maximum displacement of the vibrating object,
- m is the mass which is the mass of the pump motor, is 63 kg from *Table 4.1*.
- S is the stiffness which is the measure of how much force is required to deform the object, 680 N/mm (Toyota Material Handling, 2023b).
- α_f is the angular frequency which is the frequency of the vibration, measured in radians per second, and
- ב is the damping which is the measure of how much energy is lost during vibration, 1.5 N-s/m, (Toyota Material Handling, 2023b).

$$A = \sqrt{\frac{63 * 238.76^2 * 680}{63 * 238.76^2 + 1.5^2}}$$

$$\mathbf{A = 0.9994\ mm}$$

This means that the maximum displacement of the pump motor would be about 0.9994 mm. The amplitude of 0.9994 mm for a pump motor running at 2280 rpm is within the normal range. Thus, there is no need to worry about premature wear and tear on the pump motor. Moreover, since the new location of the pump rest on the counterweight, it further reduce the effect.

4.3. Relocating Hydraulic tank

Hydraulic reservoirs store the fluid necessary for the operation of hydraulic systems (powermotiontech, 2023). In addition to reserving enough fluid to supply a system's varying needs, hydraulic tank also provide (powermotiontech, 2023; stuffworking, 2023):

- A large surface area to transfer heat from the fluid to the surrounding environment,

- Enough volume to let returning fluid slowdown from a high entrance velocity,
- A physical barrier that separates inlet fluid from return fluid,
- Air space above the fluid to accept air that bubbles out of the fluid,
- Access to remove used fluid and contaminants, and to add new fluid, and
- A convenient surface to mount other system components, if practical.

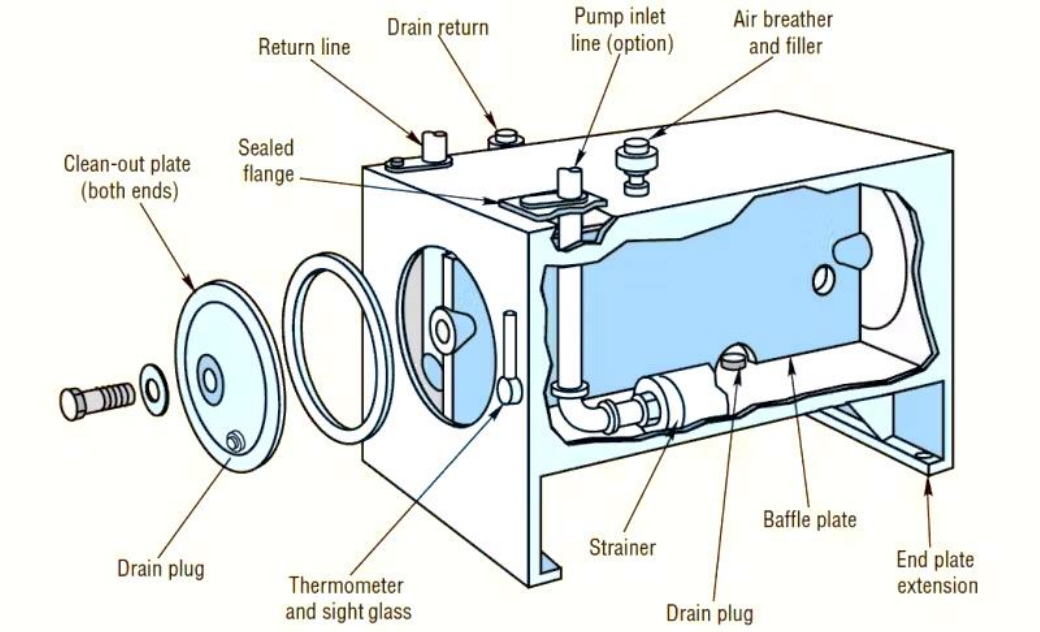

Figure 4.12: Basic components of hydraulic tank (powermotiontech, 2023)

The hydraulic tank of a forklift has several basic components as shown in *Figure 4.12*, including the suction line, return line, access plate, suction strainer, baffle plate, breather, oil level gauge, and filler cap. The suction line connects the hydraulic tank to the pump, while the return line brings the hydraulic fluid back to the tank. The access plate is for cleaning the tank, while the suction strainer filters the hydraulic fluid before it goes to the pump. The baffle plate separates the fluid into different chambers to allow for cooling and settling of contaminants. The breather is for equalizing air pressure when the fluid level changes, and the oil level gauge shows the level of oil. The filler cap is for topping up the hydraulic oil (stuffworking, 2023).

When sizing a hydraulic reservoir, the first variable to determine is the volume. The National Fluid Power Association (NFPA) suggests that the reservoir's volume should be three times the rated output of the system's fixed-displacement pump or the mean flow rate of its variable-displacement pump. This volume allows the fluid to rest between work cycles for heat dissipation, contaminant settling, and deaeration. Additionally, the reservoir should have additional space equal to at least 10% of its fluid capacity to accommodate thermal expansion and gravity drain-back during shutdown, while still providing a free fluid surface for deaeration (powermotiontech, 2023). If the reservoir is undersized, it can create a whirlpool effect at the pump's inlet, affecting the Net Positive Suction Head Required (NPSHR) and causing cavitation. Cavitation is the formation of vapor cavities in a liquid due to a change in pressure, leading to intense shockwaves, high vibration, and mechanical damage (Gannon, 2015).

The typical reservoir is constructed of welded steel plate and is designed to store and cool the fluid that supplies the system. There are three standard reservoir designs commonly used today. Joint Industry Conference (JIC), L-Shaped tank, and Overhead Stack (Gannon, 2015).

- The JIC tank is a horizontal tank with extensions that hold the tank a minimum of 6 inches off the floor.
- The L-Shaped tank is a vertical tank mounted to one side of a wide base where the pump and motor are mounted.
- The Overhead Stack is a horizontal tank mounted on a rack above the pump and motor.

The main reason for designing the tank bottom off the floor in hydraulic reservoirs is to allow for heat dissipation. It is important to ensure free airflow around the tank to prevent overheating. It is not recommended to enclose a power unit as it restricts heat dissipation (powermotiontech, 2023).

Hydraulic reservoirs are available in various design configurations, including rectangular reservoirs that have a hydraulic power unit comprised of a pump, electric motor, and other

components mounted on top of the hydraulic reservoir tank. The reservoir should contain additional space equal to at least 10% of its fluid capacity to accommodate thermal expansion and gravity drain-back during shutdown, yet still provides a free fluid surface for deaeration (Gannon, 2015).

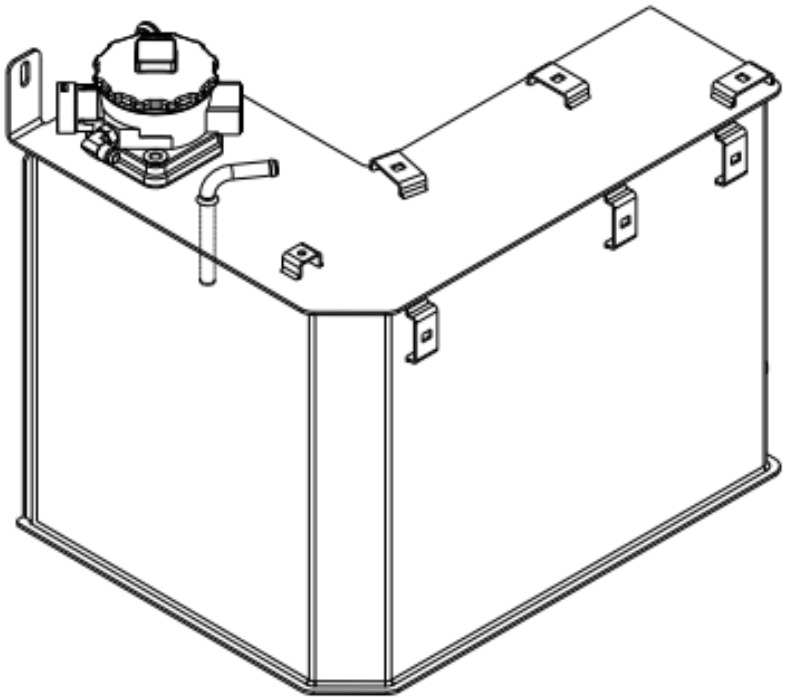

Figure 4.13: Hydraulic tank of 8FBM 40 Toyota Electric Forklift

According to the Toyota product literature, the hydraulic tank capacity of the 8FBMT40 Toyota electric forklift is 30 liters. The hydraulic oil used are AZOLLA 32 and Rando HD 32 with the density of 875 Kg/m^3 and 870 Kg/m^3, respectively.

$$m_o = \rho_o V_t \qquad \text{Equation 4-15}$$

$$m_o = 875\ kg/m^3 * 0.03\ m^3$$

$$\mathbf{m_o = 26.25\ Kg}$$

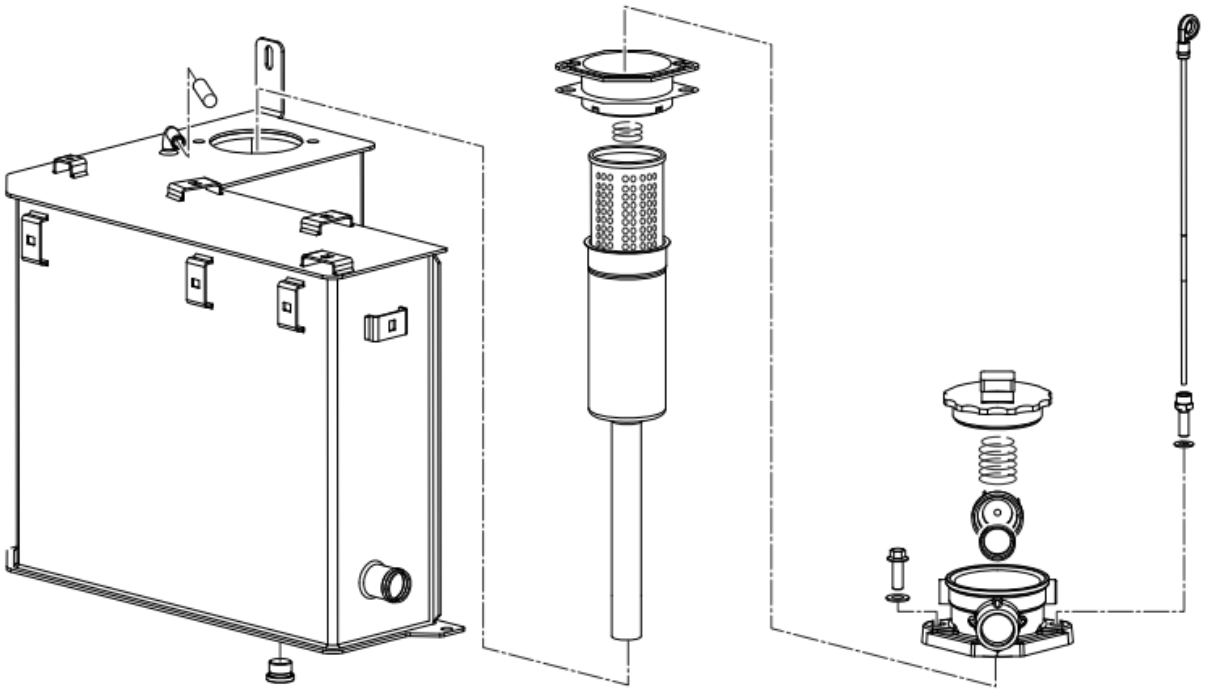

Figure 4.14: Detailed view of hydraulic tank of 8FBM 40 Toyota Electric Forklift

With few kg of weight clearance for the container, the weight of the tank is estimated to be 30 kg. In order to relocate the hydraulic tank, the available space for the relocation is option 3 as of *Figure 4.8*. The relocation of the hydraulic tank should follow as of such arrangement. This could be done in three steps. These are:

- Step 1: Removing the hydraulic tank from the front axle:

With the current installation or arrangement, hydraulic tank is on the front axle. Thus, to relocate the hydraulic tank, it is required to remove the hydraulic tank from this place. Hence, without the hydraulic tank, the weight on the front axle will be:

$$W_{nf2} = W_{ofht} - W_{ht} \qquad \text{Equation 4-16}$$

Where:

- W_{nf2} is the weight on the front axle after hydraulic tank is removed,

- W_{ofht} is the weight on the front axle before hydraulic tank is removed, and
- W_{ht} is the weight of hydraulic tank.

$$W_{nf2} = 707.411 \ - \ 30$$

$$\mathbf{W_{nf} = 677.411\ Kg}$$

Thus, after the hydraulic tank is removed, the weight on the front axle become 677.411 Kg.

- Step 2: Counterbalancing the weight removed from front axle:

Since the hydraulic tank is removed from the front axle, it is required to counterbalance the weight. This can be done in two ways. The first one is to replace the same weight as that of removed weight in the hydraulic tank place. The second one is removing the same amount of weight from the rear axle. This means removing the weight from the counterweight. Since the hydraulic tank is going to be in this place and reducing the weight is more economical than adding the weight, the second option is more feasible. Thus, the weight on the rear axle will be:

$$W_{nr2} = W_{orht} \ - \ W_{ht} \qquad \text{Equation 4-17}$$

Where:

- W_{nr2} is the weight on the rear axle after hydraulic tank is removed from front axle,
- W_{orht} is the weight on the rear axle before hydraulic tank unit is removed, and
- W_{ht} is the weight of the hydraulic tank.

$$W_{nr2} = 3{,}663.589 \ - \ 30$$

$$\mathbf{W_{nr} = 3{,}633.589\ Kg}$$

Thus, after the hydraulic tank is removed from the front axle, the weight on the rear axle become 3,633.589 Kg.

- Step 3: Relocating the hydraulic tank

As indicated on *Figure 4.8*, and discussed above, the viable option for relocating the hydraulic tank is option 3. However, option 3 puts the load on the rear axle. Therefore, to relocate the hydraulic tank without affecting the stability of the forklift, we need to remove similar weight as that of hydraulic tank. Thus, since hydraulic tank weighs 30 Kg, 30 kg of mass should be removed from the rear axle. Thus, the weight on the rear axle will be:

$$W_{nr3} = W_{nr2} - W_{ht} \qquad \text{Equation 4-18}$$

Where:

- W_{nr3} is the weight on the rear axle after removing weight for relocating hydraulic tank,
- W_{nr2} is the weight on the rear axle after hydraulic tank is removed from front axle, and
- W_{pm} is the weight of hydraulic tank.

$$W_{nr3} = 3{,}633.589 - 30$$

$$\mathbf{W_{nr1} = 3{,}603.589\ Kg}$$

Thus, after the hydraulic tank is removed from the front axle, the weight on the rear axle become 3,603.589 Kg.

Therefore, without affecting the stability of the forklift, another 60 Kg of weight is needed to be removed from the rear axle, without affecting the functionality of the components, as shown in *Figure 4.11*. However, there are four basic assemblies which their weight affect the load on the rear axle, as shown in *Figure 4.5*. These are battery pack, rear axle assembly, rear chassis and counterweight. This is from those assemblies and components, the only possible way to remove weight is from the counterweight. Currently, after relocating the pump motor unit, counterweight has a weight of 435 Kg. Thus, the new weight of the counterweight, W_{ncw1} can be determined from:

$$W_{ncw1} = 465 - 60$$

$$\mathbf{W_{ncw1} = 405\ Kg}$$

Therefore, after relocating the hydraulic tank, the new counterweight of the forklift weighs only 405 Kg.

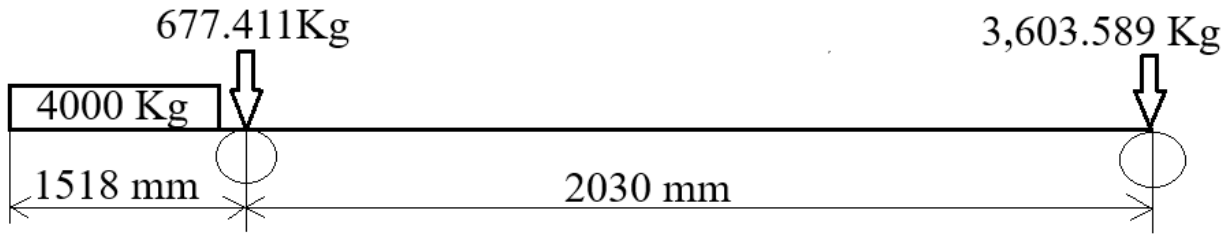

Figure 4.15: Weight distribution of the new design after hydraulic tank relocation

4.4. Hydraulic oil cooler design

Hydraulic oil cooler are just heat exchangers that facilitate exchange of heat between the two fluids that are at different temperatures while keeping them from mixing with each other. Heat exchangers are commonly used in practice in a wide range of applications, from heating and air-conditioning systems in a household, to chemical processing and power production in large plants. Heat transfer in a heat exchanger usually involves convection in each fluid and conduction through the wall separating the two fluids (Cengel & Ghajar, 2015).

Thus, hydraulic oil cooler design is the process of developing a cooler that meets the specific requirements of a hydraulic system (American Industrial Heat Transfer Inc., 2004). Different heat transfer applications require different types of hardware and different configurations of heat transfer equipment. There are two main types of hydraulic coolers. These are air-cooled and water-cooled (American Industrial Heat Transfer Inc., 2000). Air-cooled coolers are more common and less expensive, but they are not as effective as water-cooled coolers (American Industrial Heat Transfer Inc., 2004). Water-cooled coolers are more expensive, but they are more effective and can be used in applications where there is a risk of fire or explosion (American Industrial Heat Transfer Inc., 2000). Among various types of heat

exchangers Crossflow heat exchangers are usually used for vehicle applications as a cooler or radiator (Cengel & Ghajar, 2015).

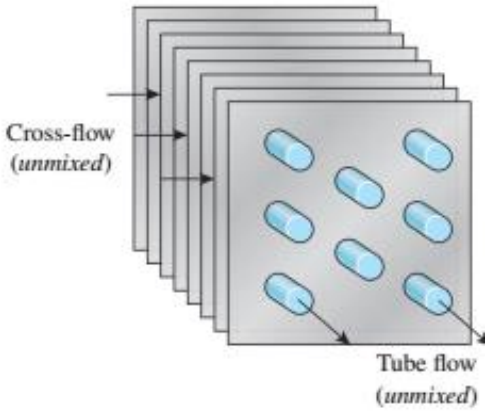

Figure 4.16: Crossflow heat exchangers (Cengel & Ghajar, 2015)

Air-cooled coolers use a fan to circulate air through the cooler core. Water-cooled coolers use a pump to circulate water through the cooler core. The fan or pump must be sized to provide enough airflow or water flow to meet the heat load requirements (American Industrial Heat Transfer Inc., 2000).

Typical hydraulic systems consisting of pumps, hydraulic lines, valves, and actuators all have inefficiencies. Even a well-designed hydraulic system will have inefficiencies when converting mechanical energy into fluid power. These issues, in addition to design and operational inefficiencies, transform some of the input power into heat. The entire system will overheat if this heat load is not dissipated. Extreme temperatures cause the fluid to overheat, reducing viscosity and eventually breaking down the fluid properties. This leads to damaged seals, bearings and excessive wear on pumps and other components. A properly sized oil cooler is required in the hydraulic system to avoid heating problems and expensive downtime due to system failure.

To properly size hydraulic oil cooler, the first procedure is to determine the heat duty. The heat duty of the cooler can be determined from:

$$Q = \dot{m}_i Cp_i \Delta T_i = \dot{m}_o Cp_o \Delta T_o \qquad \text{Equation 4-19}$$

Where:

- Q is the heat transfer flow rate,
- $\dot{m}_i$ is the mass flow rate of the inside fluid,
- $\dot{m}_o$ is the mass flow rate of the outside fluid,
- Cp_i is the specific heat of the of the inside fluid,
- Cp_o is the specific heat of the of the outside fluid,
- ΔT_i is the temperature change of the inside fluid, and
- ΔT_o is the temperature change of the outside fluid.

The required temperature of the hydraulic oil at the tank is 28℃ and the temperature of the hydraulic oil that returns from hydraulic system via return valve is 45℃ (Toyota Material Handling Company, 2015). Thus, taking the property of the oil from *Table 4.8*, the heat duty is:

$$Q = \dot{m}_i Cp_i \Delta T_i = \dot{m}_i Cp_i (T_{i1} - T_{i2})$$

$$Q = (875 * 0.0015) * 2.418 * (45 - 28)$$

$$\mathbf{Q = 53.95\ kW}$$

Then, taking the mass flow rate of the ambient air to be 5 Kg/s, and the inlet ambient air to be at 25℃, and taking the property of the air from *Table 4.9*, the exit temperature of the ambient air can be determined from *Equation 4-19*,

$$\Delta T_o = (T_{o2} - T_{o1}) = \frac{Q}{\dot{m}_o Cp_o}$$

$$T_{o2} = T_{o1} + \frac{Q}{\dot{m}_o Cp_o}$$

$$T_{o2} = 25 + \frac{53.95}{5 * 1.0063}$$

$$\mathbf{T_{o2} = 35.72℃}$$

Table 4.9: Properties of ambient air at atmospheric condition

S.No.	Property	Air
1	Density (Kg/m^3)	1.1845
2	Kinematic viscosity (mm^2/s)	15.71
3	Dynamic viscosity (mPa-s)	0.000001844
4	Specific heat at constant pressure (KJ/KgK)	1.0063
5	Thermal conductivity (w/mK)	0.0259
6	Prandtl Number	0.7296

There are two analysis method when designing a heat exchanger. These are Effectiveness – Number of Transfer of Unit ($\varepsilon - NTU$) analysis Method, and Log Mean Temperature Difference (LMTD) analysis method. The $\varepsilon - NTU$ method is particularly useful when the fluid inlet and outlet temperatures are not available, or when the flow arrangements of the heat exchanger are complex. It involves calculating the effectiveness of the heat exchanger as a function of the NTU, which is a measure of the heat transfer capacity of the exchanger. The method allows for the evaluation of heat exchanger performance and the determination of the required surface area for a given heat transfer rate.

On the other hand, the LMTD method is commonly used when the fluid inlet and outlet temperatures are known or can be easily determined. It relies on the concept of the LMTD to calculate the rate of heat transfer in heat exchangers, particularly in counter current arrangements. The LMTD method assumes constant fluid properties and provides a straightforward approach to calculate the rate of heat transfer, especially in simpler flow arrangements (Cengel & Ghajar, 2015).

Thus, for counter flow heat exchangers, using LMTD method:

$$\Delta T_{lm,CF} = \frac{\Delta T_1 - \Delta T_2}{\ln(\Delta T_1 / \Delta T_2)} \qquad \text{Equation 4-20}$$

Where:

- $\Delta T_{lm,CF}$ is the LMTD for counter flow heat exchangers,
- ΔT_1 is the temperature difference between the fluid at inlet, and
- ΔT_2 is the temperature difference between the fluid at exit.

For counter flow heat exchangers, the temperature difference between the two fluids at inlet and exit can be determined as of *Figure 4.17*.

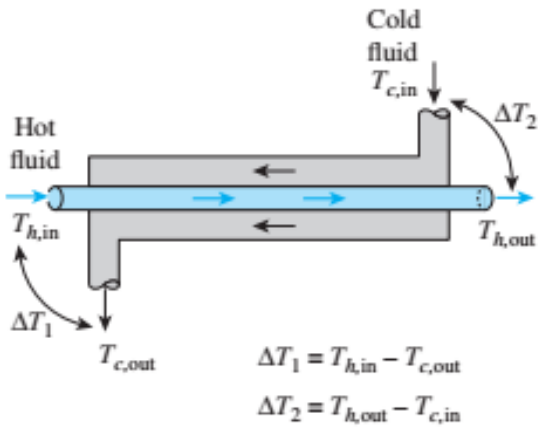

Figure 4.17: Counter flow heat exchangers (Cengel & Ghajar, 2015)

$$\Delta T_1 = T_{h1} - T_{c2} = T_{i1} - T_{o2}$$

$$\Delta T_1 = 45 - 35.72$$

$$\mathbf{\Delta T_1 = 9.277}$$

$$\Delta T_2 = T_{h2} - T_{c1} = T_{i2} - T_{o1}$$

$$\Delta T_2 = 28 - 25$$

$$\mathbf{\Delta T_2 = 3}$$

Then,

$$\Delta T_{lm,CF} = \frac{9.277 - 3}{\ln(9.277/3)}$$

$$\Delta T_{lm,CF} = \mathbf{5.56}℃$$

Crossflow heat exchangers are designed with the flow of fluids perpendicular to each other. The choice of flow arrangement depends on the required exchanger effectiveness, exchanger construction type, upstream and downstream ducting, packaging envelope, and other design criteria. In these heat exchangers, the fluids flow in perpendicular directions, with one fluid passing through the tubes while the other flows across them. Thus, both internal and external flow should be considered separately.

4.4.1. Internal flow – hydraulic oil

Internal flow plays a crucial role in the design of crossflow heat exchangers. The design of the internal flow path is essential for optimizing heat transfer and minimizing pressure drop. Factors such as tube layout, tube diameter, and flow velocity significantly impact the heat transfer efficiency (R.K.Shah & D.P.Sekulic, 2003). The flow can be either laminar or turbulent, and the type of flow will depend on the Reynolds number of the fluid. In laminar flow, the fluid flows in smooth, parallel layers. This type of flow is characterized by low heat transfer rates and low pressure drops. In turbulent flow, the fluid flows in a chaotic manner. This type of flow is characterized by high heat transfer rates and high pressure drops (H.Liu et al., 2012).

Generally, Crossflow heat exchangers have the tube diameter ranging from 5 to 55 mm, and tube length ranging from 100 to 1000 mm. The specific dimensions of the tubes will be determined by the heat transfer requirements of the application, the pressure drop that can be tolerated, the cost of the materials, and the availability of the materials. For example, a radiator in a car engine would typically have smaller tubes with a shorter length than a radiator in a large building (R.K.Shah & D.P.Sekulic, 2003). This is because the car engine needs to dissipate heat quickly, while the building radiator can use larger tubes and a longer length to achieve the desired heat transfer rate (American Industrial Heat Transfer Inc.,

2000). However, heat exchangers with small diameter and large length have better effectiveness. Thus, let's take a tube with $d_o = 25\ mm$, $d_i = 19\ mm$ and $L_t = 900\ mm$.

Flow velocity

The flow velocity for internal flow in the crossflow heat exchangers can be determined from:

$$v_i = \frac{\dot{m}_i}{\rho_i A_i} = \frac{\dot{V}_i}{\left(0.25\pi {d_i}^2\right)} \qquad \text{Equation 4-21}$$

Where:

- v_i is the velocity of the fluid inside the tube,
- $\dot{V}_i$ is the volume flow rate of the fluid inside the tube, and
- d_i is the inner tube diameter.

$$v_i = \frac{0.0015}{(0.25 * \pi * 0.019^2)}$$

$$\mathbf{v_i = 5.293\ m/s}$$

Reynolds number

The Reynolds number is a dimensionless quantity that is used to characterize the flow of a fluid. It is defined as the ratio of the inertial forces to the viscous forces in the fluid (H.Liu et al., 2012). The higher the Reynolds number, the more turbulent the flow (Cengel & Ghajar, 2015). The Reynolds number for internal flow in the crossflow heat exchangers can be determined from:

$$Re_i = \frac{\rho_i v_i d_i}{\mu_i} \qquad \text{Equation 4-22}$$

Where:

- Re_i is the Reynolds number of the internal flow,
- ρ_i is the density of the fluid inside the tube,

- v_i is the velocity of the fluid inside the tube,
- μ_i is the dynamic viscosity of the fluid inside the tube, and
- d_i is the inner tube diameter.

$$Re_i = \frac{875 * 5.293 * 0.019}{0.0032}$$

$$\mathbf{Re_i = 27498.8}$$

The range of Reynolds number to determine the laminar and turbulent for internal flow in tubes is (H.Liu et al., 2012):

Laminar flow: Re < 2300

Transition flow: 2300 < Re < 4000

Turbulent flow: Re > 4000

Thus, the flow is turbulent inside the tube. Then, high heat transfer rates are expected.

Nusselt number

The Nusselt number for internal flow in the crossflow heat exchangers can be determined from:

$$Nu_i = 0.023 {Re_i}^{0.8} {Pr_i}^{0.3}$$ Equation 4-23

Where:

- Nu_i is the Nusselt number of the internal flow,
- Re_i is the Reynolds number of the internal flow, and
- Pr_i is the Reynolds number of the internal flow.

$$Nu_i = 0.023(27498.8)^{0.8}(145)^{0.3}$$

$$\boldsymbol{Nu_i = 364.41}$$

Heat transfer coefficient

The heat transfer coefficient for internal flow in the crossflow heat exchangers can be determined from:

$$h_i = \frac{Nu_i k_i}{d_i} \qquad \text{Equation 4-24}$$

Where:

- h_i is the heat transfer coefficient of the internal flow,
- Nu_i is the Nusselt number of the internal flow,
- k_i is the thermal conductivity of the fluid inside the tube, and
- d_i is the inner tube diameter.

$$h_i = \frac{364.41 * 0.14}{0.019}$$

$$\mathbf{h_i = 2685\ w/m^2K}$$

Therefore, the internal flow with hydraulic oil fluid for this system has 2685 w/m^{2}K heat transfer coefficient.

4.4.2. External flow – ambient air

External flow in the design of crossflow heat exchangers refers to the flow of fluids outside the tubes. The design of the external flow path is essential for maximizing heat transfer and minimizing the overall size and cost of the heat exchanger (R.K.Shah & D.P.Sekulic, 2003). Factors such as the flow velocity, flow direction, and flow distribution across the external surface of the tubes significantly influence heat transfer efficiency (Cengel & Ghajar, 2015). The flow can be either laminar or turbulent, and the type of flow will depend on the Reynolds number of the fluid. The range of Reynolds number to determine laminar and turbulent flow for external flow on tubes depends on various factors including the geometry of the flow, fluid properties, and surface roughness (H.Liu et al., 2012). Generally, for flow over tubes,

the transition from laminar to turbulent flow occurs at a Reynolds number range of approximately 4,000 to 5,000 (R.K.Shah & D.P.Sekulic, 2003).

Flow Velocity

The flow velocity for external flow in the crossflow heat exchangers can be determined from:

$$v_o = \frac{\dot{m}_o}{\rho_o A_o} = \frac{\dot{m}_o}{\rho_o(\pi d_o L_t)}$$ Equation 4-25

Where:

- v_o is the velocity of the fluid outside the tube,
- $\dot{m}_o$ is the mass flow rate of the fluid outside the tube,
- ρ_o is the density of the fluid outside the tube,
- d_o is the outer tube diameter, and
- L_t is the tube length.

$$v_o = \frac{5}{1.1845(\pi * 0.025 * 0.9)}$$

$$\mathbf{v_o = 59.75\ m/s}$$

Reynolds number

The Reynolds number for external flow in the crossflow heat exchangers can be determined from:

$$Re_o = \frac{\rho_o v_o d_o}{\mu_o}$$ Equation 4-26

Where:

- Re_i is the Reynolds number of the external flow,
- ρ_o is the density of the fluid outside the tube,
- v_o is the velocity of the fluid outside the tube,

- μ_o is the dynamic viscosity of the fluid outside the tube, and
- d_o is the outer tube diameter.

$$Re_o = \frac{1.1845 * 59.75 * 0.025}{0.000001844}$$

$$\mathbf{Re_o = 959482}$$

Thus, the flow over the tube is turbulent. Then, high heat transfer rates are expected.

Nusselt number

The Nusselt number for external flow in the crossflow heat exchangers can be determined from:

$$Nu_o = 0.664 Re_i^{0.5} Pr_o^{0.33}$$ Equation 4-27

Where:

- Nu_o is the Nusselt number of the external flow,
- Re_o is the Reynolds number of the external flow, and
- Pr_o is the Reynolds number of the external flow.

$$Nu_o = 0.664(959482)^{0.5}(0.7296)^{0.33}$$

$$\mathbf{Nu_o = 586.14}$$

Heat transfer coefficient

The heat transfer coefficient for external flow in the crossflow heat exchangers can be determined from:

$$h_o = \frac{Nu_o k_o}{d_o}$$ Equation 4-28

Where:

- h_o is the heat transfer coefficient of the external flow,

- Nu_o is the Nusselt number of the external flow,
- k_o is the thermal conductivity of the fluid outside the tube, and
- d_o is the outer tube diameter.

$$h_o = \frac{586.14 * 0.0259}{0.025}$$

$$\mathbf{h_o = 607.25\ w/m^2K}$$

Therefore, the internal flow with hydraulic oil fluid for this system has 607.25 w/m^{2}K heat transfer coefficient.

4.4.3. Correction factor for crossflow heat exchangers

The LMTD analysis is limited to parallel-flow and counter-flow heat exchangers only. Similar relations are also developed for cross-flow heat exchangers, but the resulting expressions are too complicated because of the complex flow conditions. In such cases, it is convenient to relate the equivalent temperature difference to the LMTD relation for the counter-flow case. Thus, for counter flow heat exchangers, using LMTD method (Cengel & Ghajar, 2015):

$$\Delta T_{lm} = F \Delta T_{lm,CF} \qquad \text{Equation 4-29}$$

Where:

- ΔT_{lm} is the LMTD for crossflow heat exchangers,
- $\Delta T_{lm,CF}$ is the LMTD for counter flow heat exchangers, and
- F is the correction factor for crossflow heat exchangers.

The correction factor depends on the geometry of the heat exchanger and the inlet and outlet temperatures of the hot and cold fluid streams. The correction factor is less than unity for a cross-flow heat exchanger. Thus, the correction factor is a measure of deviation of the LMTD from the corresponding values for the counter-flow case (H.Liu et al., 2012).

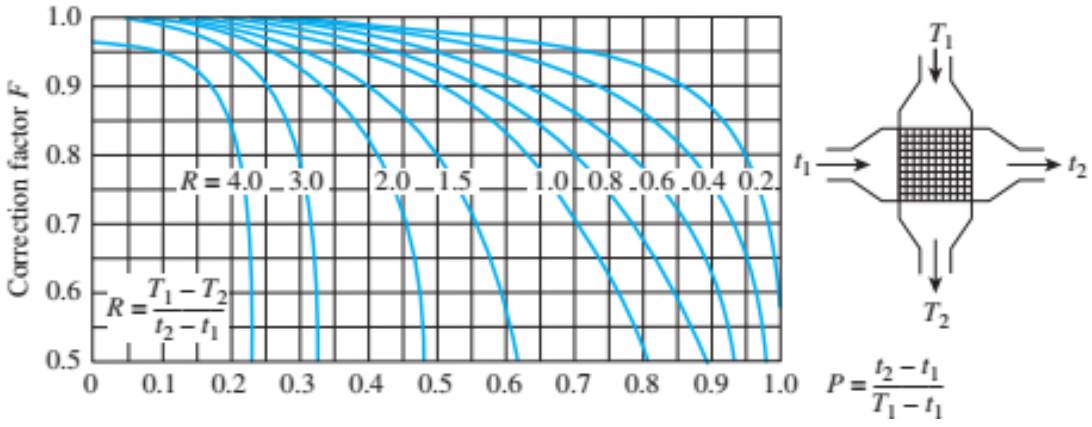

Figure 4.18: Correction factor for cross-flow heat exchangers (Cengel & Ghajar, 2015)

$$R = \frac{T_{i1} - T_{i2}}{T_{o2} - T_{o1}} = \frac{45 - 27}{43.88 - 25} = \mathbf{1.585}$$

$$P = \frac{T_{o2} - T_{o1}}{T_{i1} - T_{o1}} = \frac{43.88 - 25}{45 - 25} = \mathbf{0.536}$$

From *Figure 4.18* using R and P, the correction factor will be:

$$\boldsymbol{F@\begin{cases} R = 1.585 \\ P = 0.536 \end{cases} = 0.75}$$

4.4.4. Overall heat transfer coefficient

Then, the overall heat transfer coefficient can be determined from:

$$\frac{1}{U_o} = \frac{1}{h_i} + \frac{1}{h_o}$$ Equation 4-30

Where:

- U_o is the overall heat transfer coefficient,
- h_i is the heat transfer coefficient of the internal flow, and
- h_o is the heat transfer coefficient of the external flow.

$$\frac{1}{\mathrm{U_o}} = \frac{1}{2685} + \frac{1}{607.25}$$

$$\mathbf{U_o = 495.25\ w/m^2K}$$

4.4.5. Total surface area of the exchanger

Then, the total surface area required for the heat transfer can be determined from:

$$A_s = \frac{Q}{U_o F \Delta T_{lm}} \qquad \text{Equation 4-31}$$

Where:

- A_s is the surface area of the heat exchanger,
- Q is the heat transfer flow rate,
- U_o is the overall heat transfer coefficient,
- F is the correction factor for crossflow heat exchanger, and
- ΔT_{lm} is the LMTD for counter flow heat exchangers.

$$A_s = \frac{53951}{495.25 * 0.75 * 5.56}$$

$$\mathbf{A_s = 26.12\ m^2}$$

4.4.6. Total length of the tube

Here, the total length of the tube can be determined from:

$$L = \frac{A_s}{\pi d_o} \qquad \text{Equation 4-32}$$

Where:

- L is the total length of the tube.
- A_s is the surface area of the heat exchanger, and
- d_o is the tube outside diameter.

$$L = \frac{26.12}{\pi * 0.025}$$

$$\mathbf{L = 332.78\ m}$$

4.4.7. Number of tubes

Then, the number of tubes can be calculated from:

$$N_t = \frac{L}{L_t} \qquad \text{Equation 4-33}$$

Where:

- N_t is the number of tubes,
- L is the total length of the tube, and
- L_t is the length of single tube.

$$N_t = \frac{\mathbf{332.78}}{0.9}$$

$$\mathbf{N_t \approx 370}$$

Thus, the exchanger is expected to have 370 tubes with 0.019 m, 0.025 m and 0.9 m inner diameter, outer diameter and length, respectively. The summary of the input parameters, the fluid properties, the design geometries and configurations, and the output parameters are presented in *Table 5.1 and Therefore*, without affecting the stability of the forklift, another 165.18 Kg of weight is needed to be removed from the rear axle. Currently, after relocating the pump motor unit and hydraulic tank, counterweight has a weight of 405 Kg. Thus, the new weight of the counterweight, W_{ncw2} can be determined from:

$$\mathrm{W_{ncw2}} = 405 - 165.18$$

$$\mathbf{W_{ncw2} = 239.82\ Kg}$$

Therefore, after incorporating the cooler, the new counterweight of the forklift weighs only 239.82 Kg..

As such, since the cooler is included in the design, the weight of this cooler is needed to be calculated. Then, neglecting the plate weight and instant air weight, the weight of the cooler can be calculated from:

$$W_C = W_{hx} + W_{oil} = 0.25\pi L\{[\rho_{hx}(d_o - d_i)^2] + [\rho_{oil} d_i{}^2]\}$$ Equation 4-34

Where:

- W_C is the weight of the cooler,
- W_{hx} is the weight of the heat exchanger,
- W_{oil} is the weight of the hydraulic oil in the heat exchanger,
- L is the total length of the tube,
- ρ_{hx} and ρ_{oil} are the density of exchanger material and oil, respectively, and
- d_o and d_i are the outer and inner tube diameter, respectively.

$$W_C = 0.25\pi * 332.78\{[8790 * (0.025 - 0.019)^2] + [875 * 0.019^2]\}$$

$$\mathbf{W_C = 165.18\ Kg}$$

Therefore, without affecting the stability of the forklift, another 165.18 Kg of weight is needed to be removed from the rear axle. Currently, after relocating the pump motor unit and hydraulic tank, counterweight has a weight of 405 Kg. Thus, the new weight of the counterweight, W_{ncw2} can be determined from:

$$W_{ncw2} = 405 - 165.18$$

$$\mathbf{W_{ncw2} = 239.82\ Kg}$$

Therefore, after incorporating the cooler, the new counterweight of the forklift weighs only 239.82 Kg.

4.5. CAD Modeling

To show both the old model and new model after relocation of the selected component, SOLIDWORKS software is used. As discussed earlier, pump motor with hydraulic oil pump, shown in *Figure 4.19*, and hydraulic oil tank is relocated.

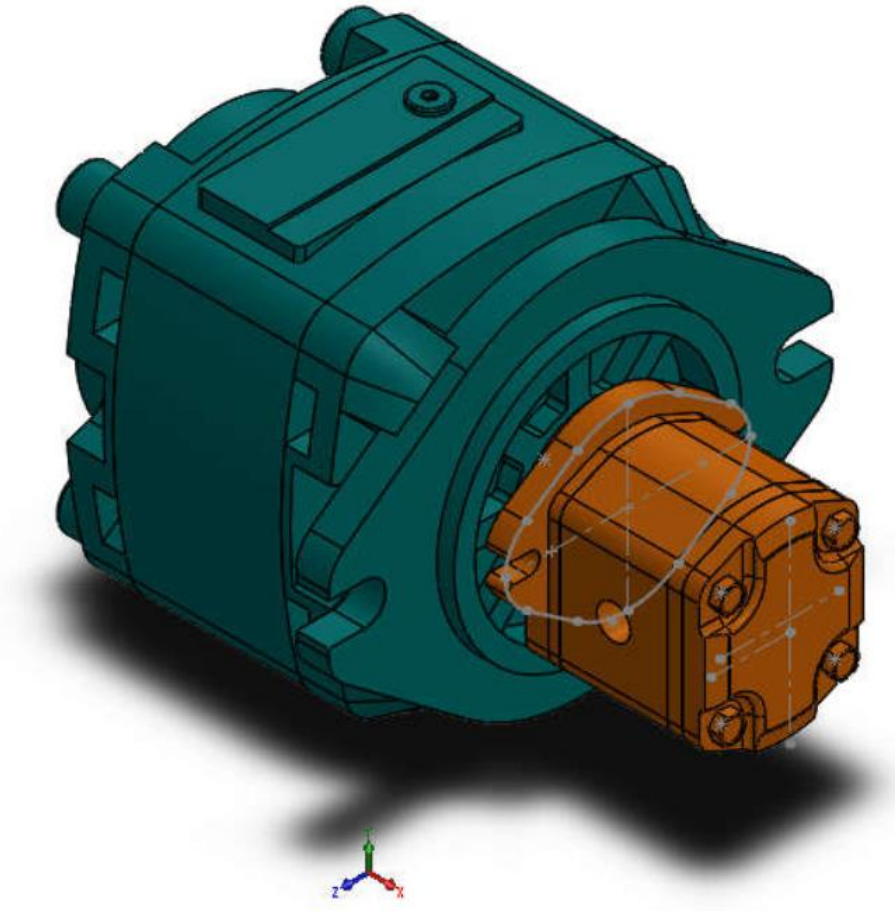

Figure 4.19: Solidworks model snap view of Pump motor with hydraulic pump

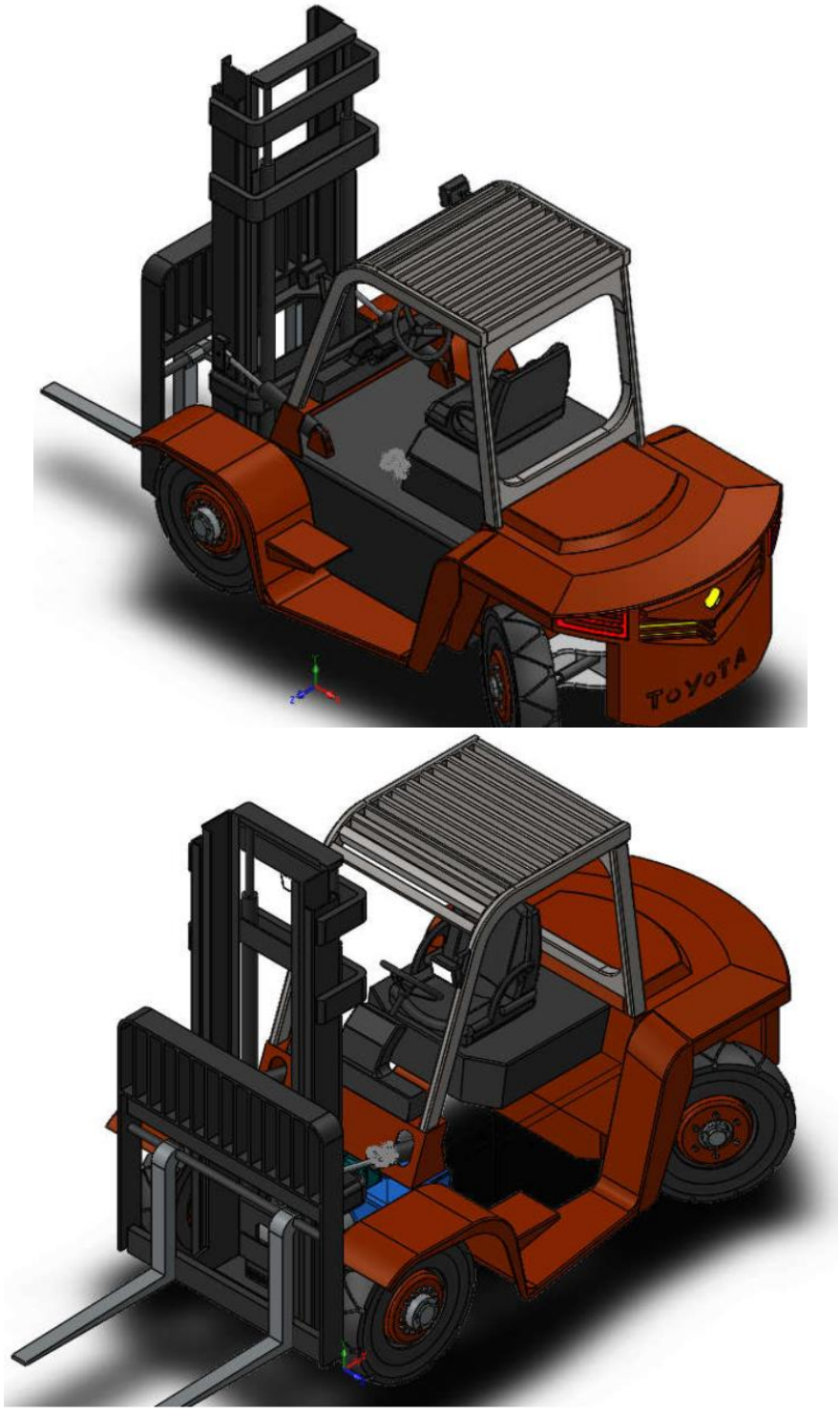

Figure 4.20: SolidWorks Isometric View of the current model

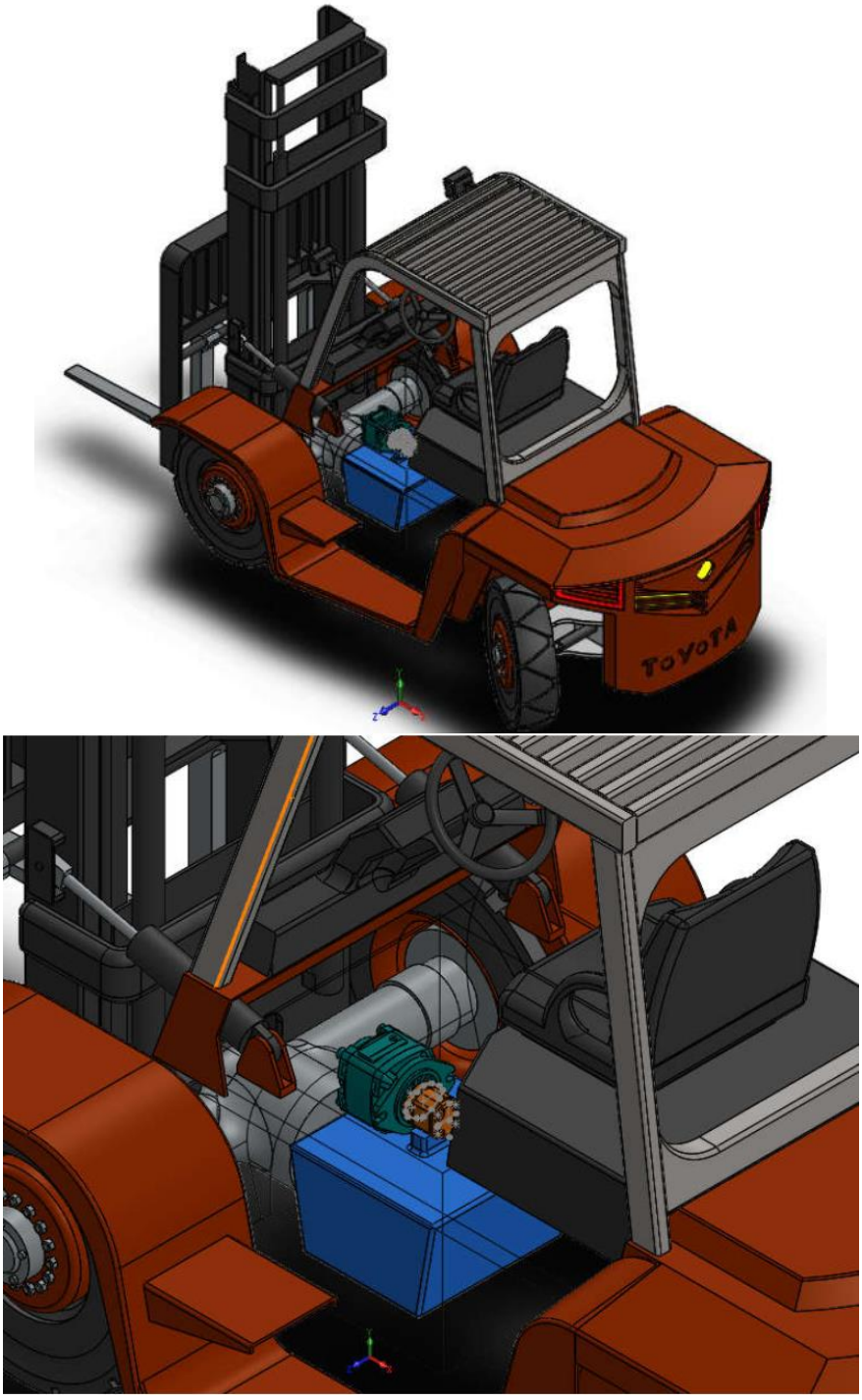

Figure 4.21: Current location of Pump motor with hydraulic pump

In the new model cooler is also incorporated, as shown in *Figure 4.22*. The SolidWorks model is created for both the current system and the new model. The model for current system is shown in *Figure 4.20* and *Figure 4.21*, whereas, the model for the new system is shown in *Figure 4.23*.

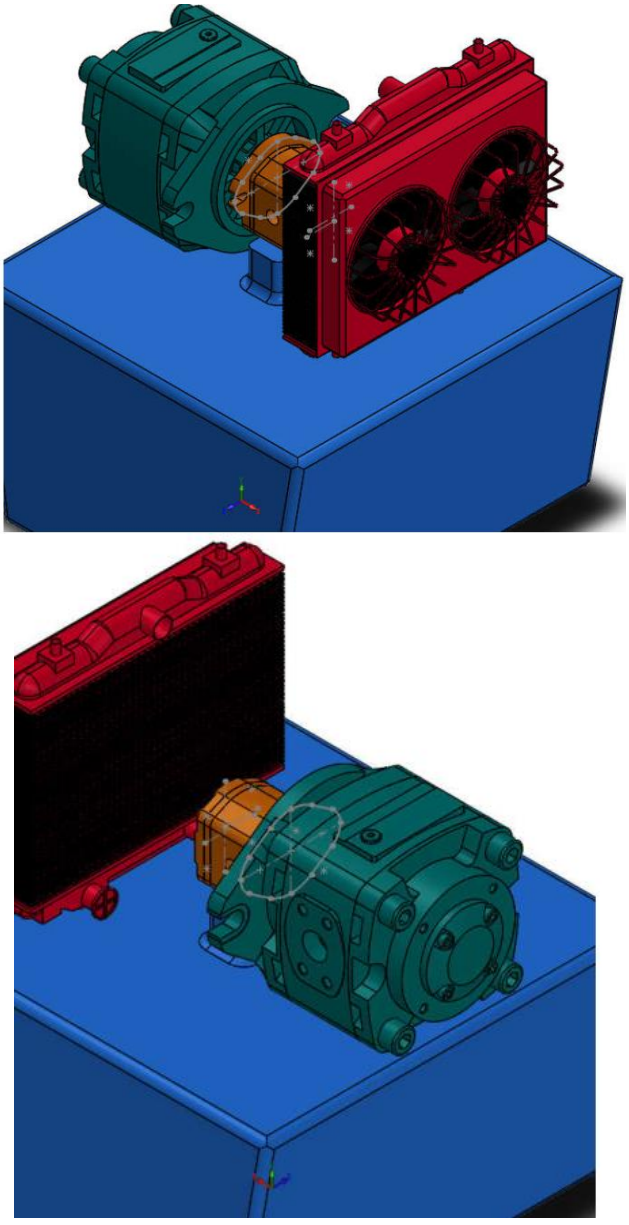

Figure 4.22: Cooler Incorporated in Pump motor assembly for the new model

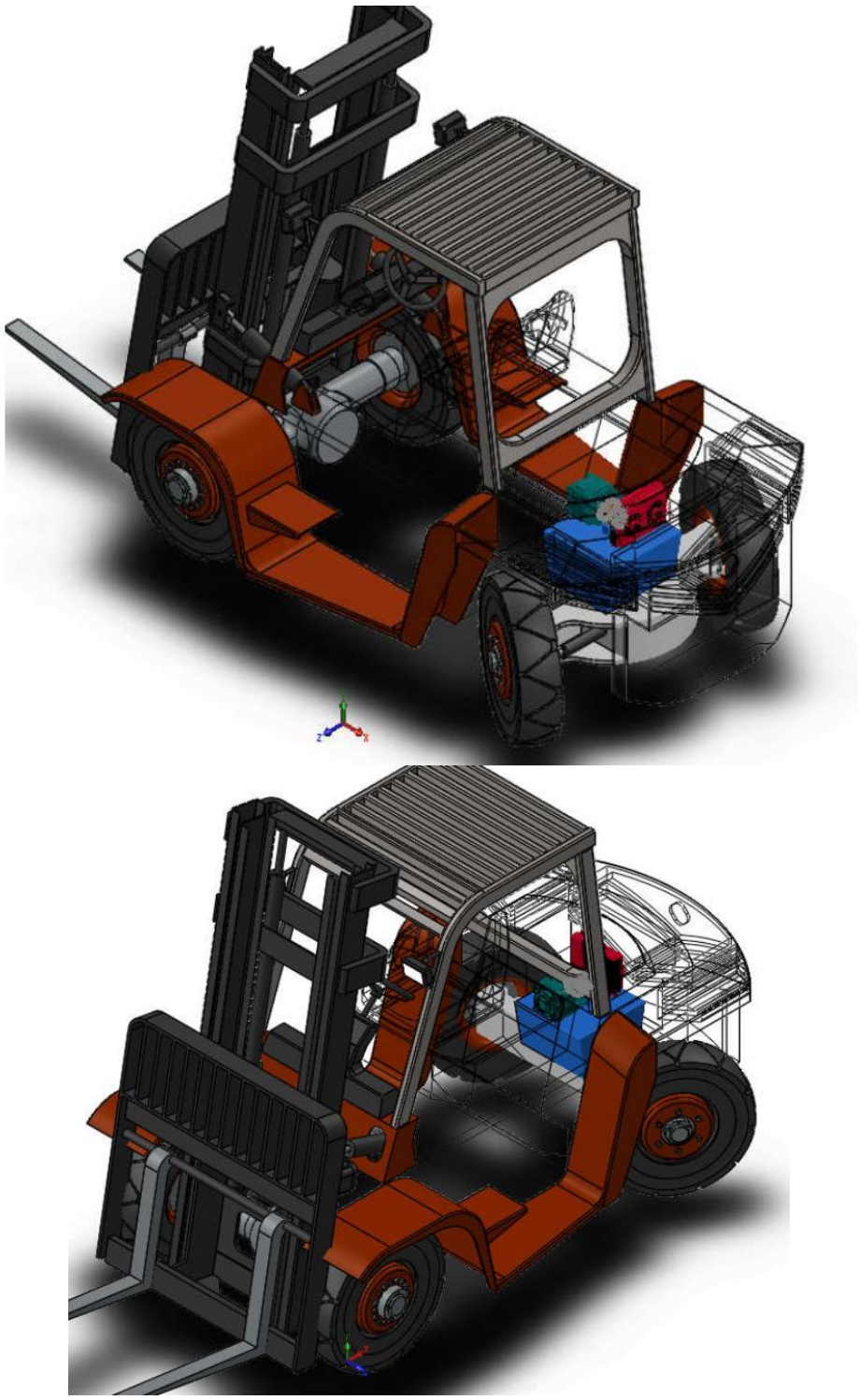

Figure 4.23: The new location of Pump motor unit

4.6. Load and Stress Analysis

The load and stress analysis is done using ANSYS static structural on the ANSYS Mechanical environment. This is done by considering the whole structure of the forklift as overhanging beam on both sides. The whole analysis is done for both the current model and the new model as follows.

4.6.1. Analysis for current Model

The analysis begins with selecting the module from ANSYS workbench. As such ANSYS Static structure is selected. This consists of six basic steps, as shown in *Figure 4.24*. And each steps used are discussed below starting with the geometry.

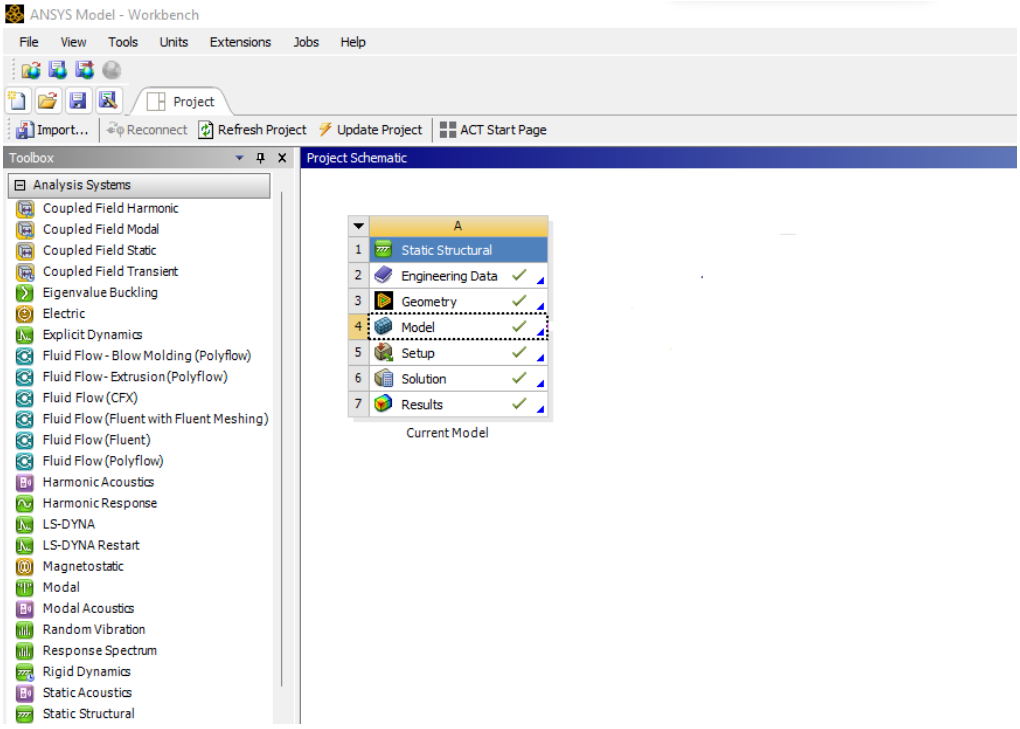

Figure 4.24: Basic steps and procedures in ANSYS static structure module

The simplified model geometry of the current forklift model is created in SolidWorks by considering the separate sections of the forklift as of the fork, mast, front axle, middle body, rear axle and counterweight, as shown in *Figure 4.25*.

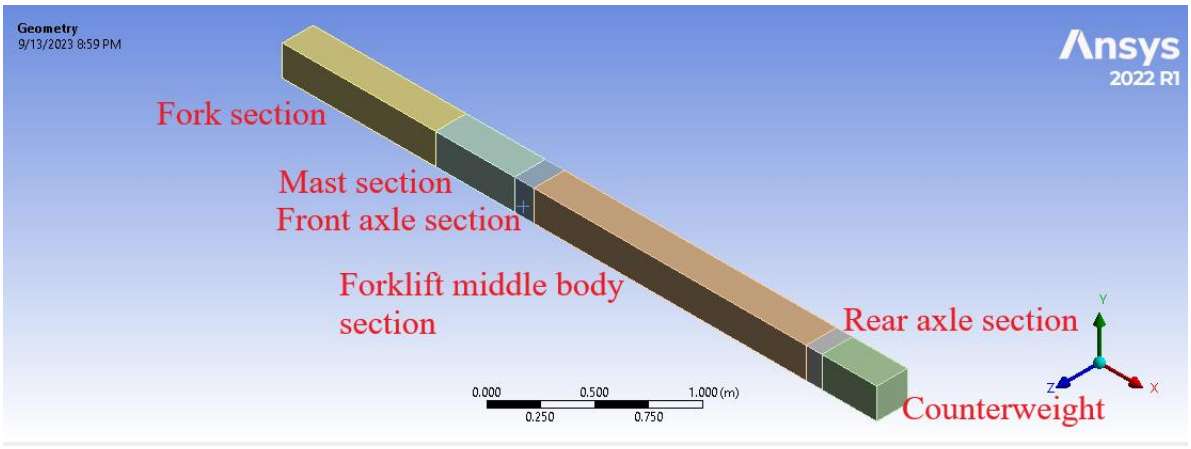

Figure 4.25: The simplified Geometry of the current model with various separate sections

Then, after the geometry is opened in a Design Modeler of ANSYS and arranged and edited as that of ANSYS's acceptance, it is opened in ANSYS Mechanical for further analysis as shown in *Figure 4.26*.

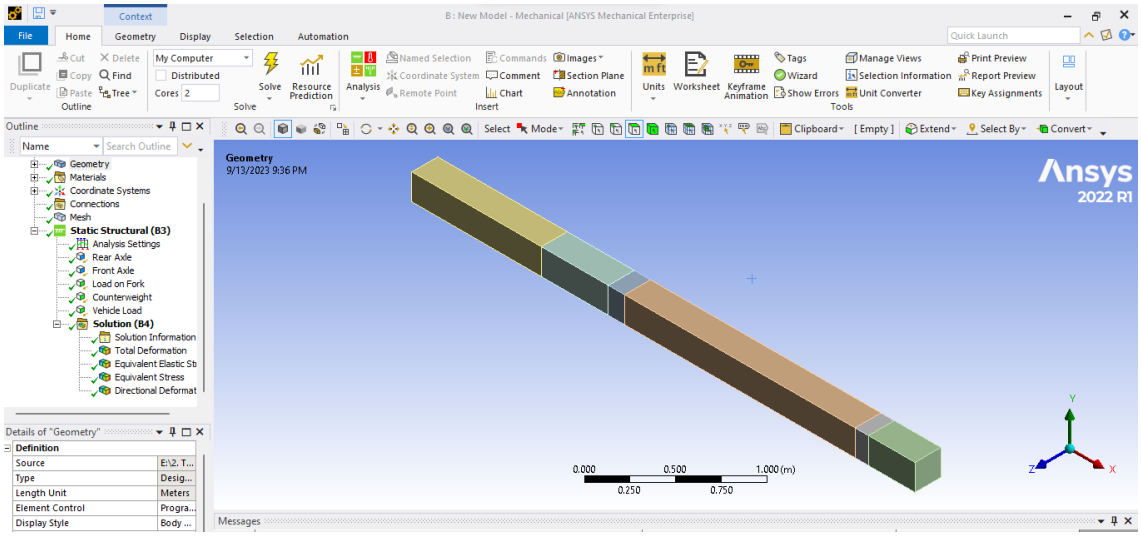

Figure 4.26: ANSYS Mechanical environment

After the setup of the geometry is completed, the next step in ANSYS Mechanical is Meshing. The meshing is performed using two processes. The first process is to apply the type of meshing method. As such Hex Dominant Method is selected for simplified and

distributed meshing. Furthermore, sizing method is applied to fine the meshing, as shown in *Figure 4.27*.

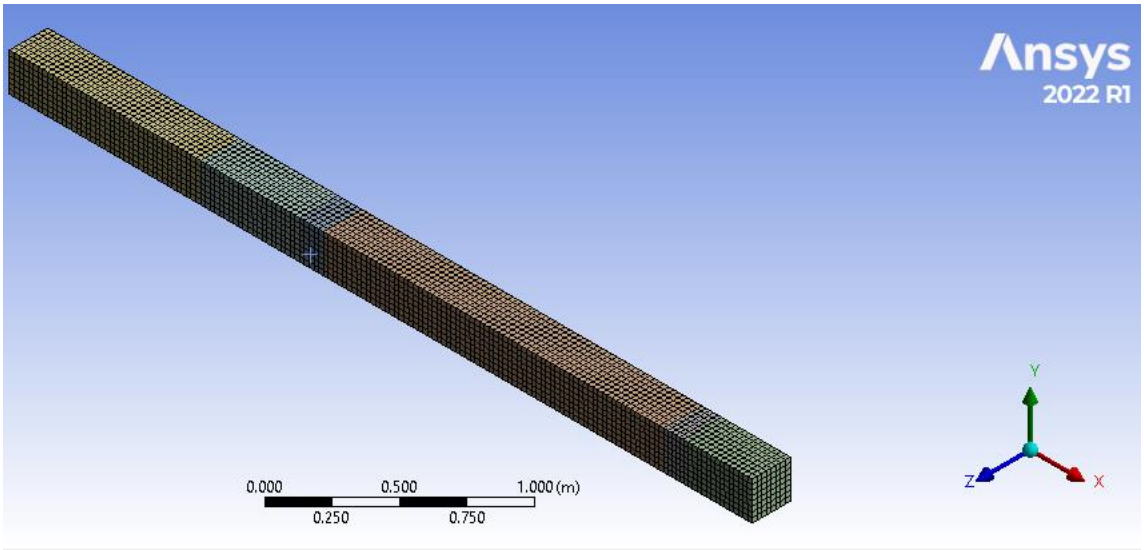

Details of "Hex Dominant Methoc

Scope	
Scoping Method	Geometry Selection
Geometry	6 Bodies
Definition	
Suppressed	No
Method	Hex Dominant
Element Order	Use Global Setting
Free Face Mesh Type	Quad/Tri
Control Messages	No

Details of "Body Sizing" - Sizing

Scope	
Scoping Method	Geometry Selection
Geometry	6 Bodies
Definition	
Suppressed	No
Type	Element Size
Element Size	2.5e-002 m
Advanced	
Defeature Size	Default
Behavior	Soft

Figure 4.27: Meshing in ANSYS Mechanical for simplified current model of the forklift

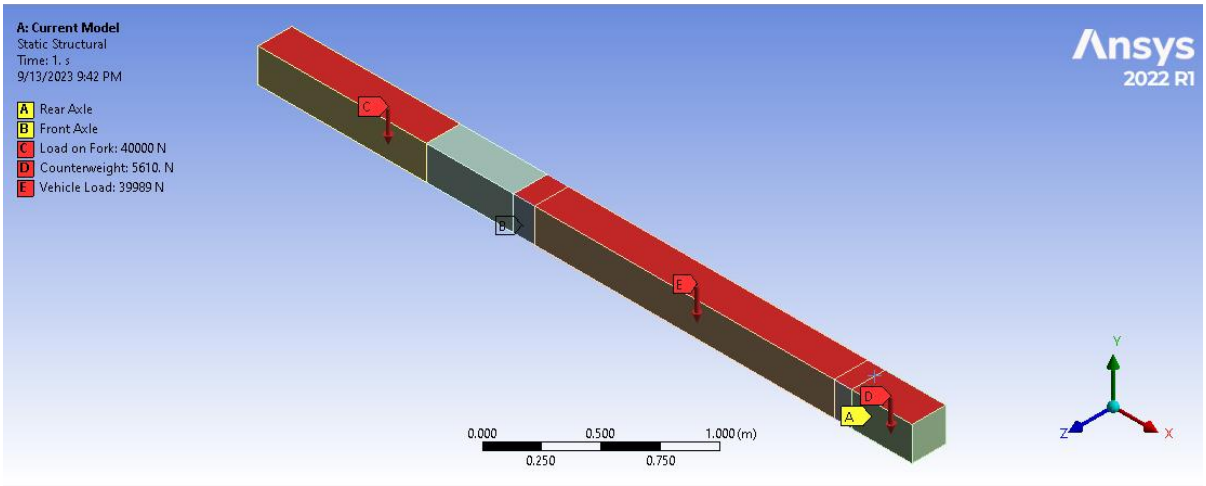

Figure 4.28: The load and the displacement on the simplified model of the current forklift

After the meshing is completed, the next step in ANSYS Mechanical is applying the constraints and the forces. For this model, two constraints are applied. These are roller constraints that can be similar to the front and rear wheels that are at front and rear axle, respectively. Whereas, the loads are considered as the load on the forklift, the counterweight and the vehicle load itself, as shown in *Figure 4.28*.

After analysis is completed, ANSYS mechanical can generate various results upon request. For this particular model, deformation, strain and stress are considered for the solution. Total deformation and directional deformation, equivalent elastic strain, and Von-Misses stress are particularly selected, as shown in *Figure 4.26*.

4.6.2. Analysis for new Model

The analysis for new model is similar with that of the current model. Thus, few steps or procedures are considered from the durrent model, as shown in *Figure 4.29*. As such, the geometry and meshing is taken from the current model analysis. Whereas, the separate analysis for the new model started from the load and displacement analysis.

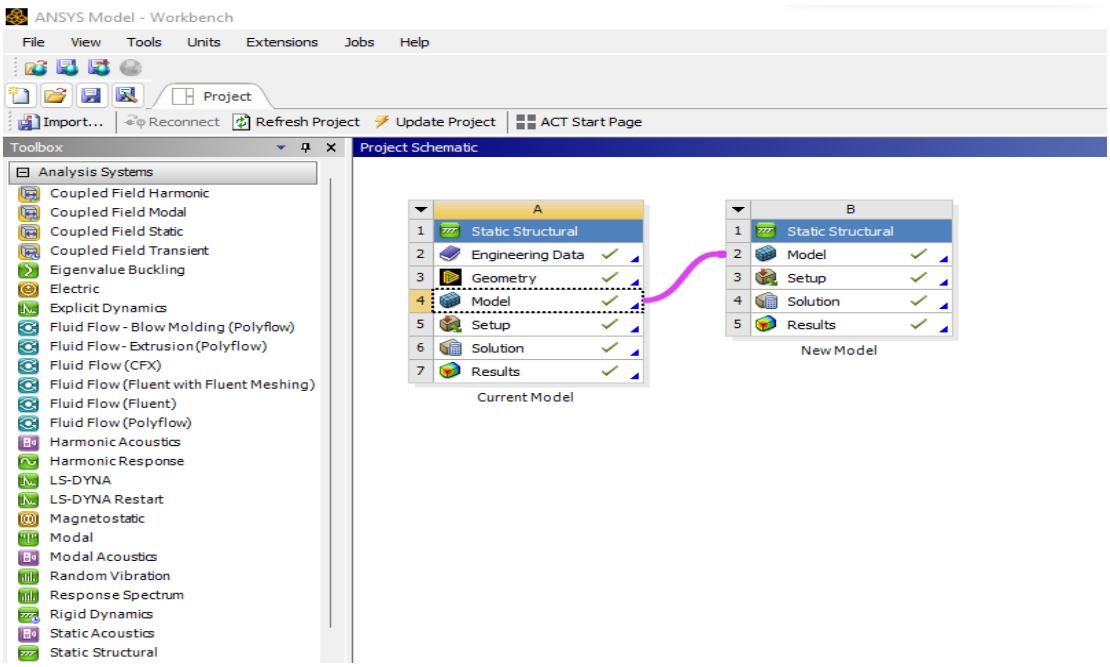

Figure 4.29: Couple steps and procedures in ANSYS static structure module

For this model, two constraints are applied. These are roller constraints that can be similar to the front and rear wheels that are at front and rear axle, respectively. Whereas, the loads are considered as the load on the forklift, the counterweight and the vehicle load itself, as shown in *Figure 4.30*.

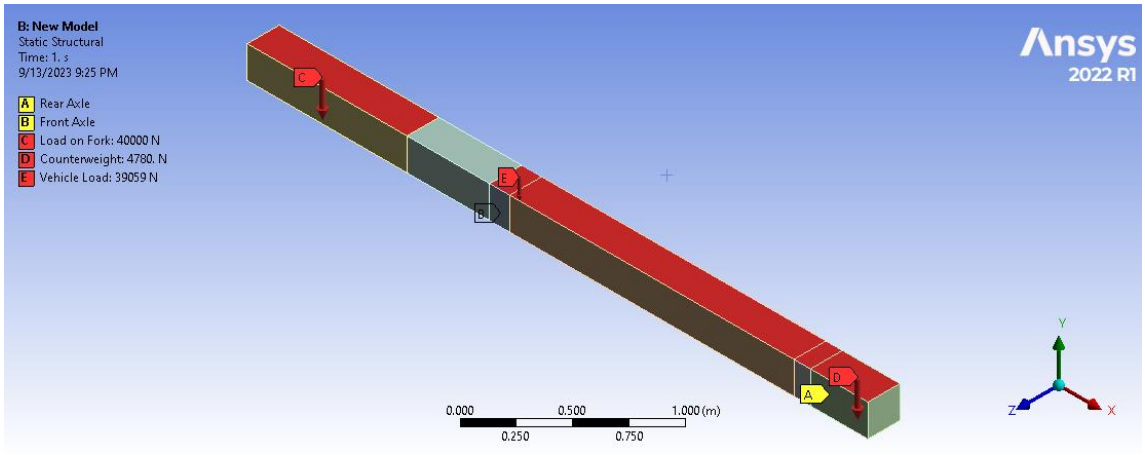

Figure 4.30: The load and the displacement on the simplified model of the new forklift

After analysis is completed, total deformation and directional deformation, equivalent elastic strain, and Von-Misses stress are particularly selected.

Chapter Five

5. Result and Discussion

For the ease of maintenance and avoiding vulnerability to external factors, 8FBM 40 Toyota Electric Forklift components relocation is performed. As such relocation of pump motor unit and hydraulic tank is designed and modeled. This is done by considering factors such as accessibility of the new location, space availability, weight distribution, vibration generated, and heat dissipation and cooling requirement of the components relocated. Based on these criteria, three new locations were identified and investigated for the relocation of the components, as shown in *Figure 4.8*. However, considering the space availability of these three identified locations, only one of the three locations has sufficient space to accommodate the intended components for relocation. Hence, option 3 which is the rear side of the forklift is selected for further analysis of the relocation of the components.

Accordingly, it is possible to obtain 96.67% of the accessibility score by relocating these components to the rear side of the forklift by removing few weights of the counterweight. This indicates, the components are accessible directly from this location. Moreover, without affecting the stability of the forklift, 186 Kg of weight is needed to be removed from the rear axle, to counter balance the pump motor unit and hydraulic tank t removed from the front axle. Therefore, after relocating the pump motor unit and hydraulic tank, the new counterweight of the forklift weighs only 405 Kg. In addition, the pump gain 1.149 ^{O}C temperature while dissipating 3.6465 kW of heat to the atmospheric air. Since this value is small, there is no risk of overheating. Furthermore, the maximum displacement of the pump motor would be about 0.9994 mm which is within the normal range for a pump motor running at 2280 rpm is within the normal range. Thus, there is no need to worry about premature wear and tear on the pump motor. Moreover, since the new location of the pump rest on the counterweight, it further reduce the effect.

Additionally, to increase the lifespan of the hydraulic oil and to reduce the operational cost of the forklift, in addition to relocating the pump motor unit and hydraulic tank, oil cooler is incorporated to the new design. The design parameters and outputs are summarized in *Table 5.1* and *Table 5.2*, respectively.

Table 5.1: Design parameters of the hydraulic oil cooler

S.No.	Parameters	Tube side	Plate Side
1	Fluid type	Hot – inlet	Cold – inlet
2	Fluid Name	Oil	Air
3	Inlet Temperature (℃)	45	25
4	Exit Temperature (℃)	28	35.72
5	Density (Kg/m^3)	875	1.1845
6	Specific heat, Cp (w/m^2K)	2418	1006.3
7	Thermal Conductivity (w/mK)	0.14	0.0259
8	Dynamic Viscosity ($mPa-s$)	0.0032	$1.844*10^{-6}$
9	Prandtl Number	145	0.7296
10	Mass flow rate (Kg/s)	1.3125	5
11	Exchanger type	Crossflow heat exchanger	
12	LMTD (℃)	5.56	
13	Correction factor	0.75	
14	Heat Duty (w)	53951	

LMTD method is selected to design the heat exchanger. The cooler is a crossflow heat exchanger with hot oil flowing on the tube side and cold air flowing on the plate side. The oil enters the cooler at a temperature of 45°C and exits at 28°C, while the air enters at 25°C. The oil cooler's design parameters depend on the type of oil, flow rate, inlet and ambient temperatures, heat load, and altitude. The LMTD and correction factor are used to calculate the heat transfer rate and the required heat exchange volume. The heat duty of the cooler is about 53 kW, which indicates the amount of heat that the cooler can dissipate from the hydraulic system.

Table 5.2: The design geometries and outputs of the hydraulic oil cooler

S.No.	Parameters	Tube side	Plate Side
1	Tube inner diameter (m)	0.019	
2	Tube outer diameter (m)	0.025	
3	Tube length (m)	0.9	
4	Velocity (m/s)	5.293	59.75
5	Reynolds Number	27499	959482
6	Nusselt Number	364.4	586.14
7	Heat transfer coefficient (w/m^2K)	2685.18	607.24
8	Overall heat transfer coefficient (w/m^2K)	495.25	
9	Surface area (m^2)	26.12	
10	Total length of tubes (m)	332.78	
11	Number of tubes	370	

The cooler has tube inner diameter of 0.019 m, tube outer diameter of 0.025 m, and a tube length of 0.9 m. The plate side has a velocity of 59.75 m/s, and the total length of tubes is 332.78 m with 370 tubes. The tube side has a smaller diameter and length than the plate side. This is because the tube side is typically used for the hot fluid, which needs to be more efficiently cooled. The tube side has a higher Reynolds number than the plate side which indicates a higher Reynolds number indicates more turbulence. Turbulence helps to improve the heat transfer coefficient.

As such, since the cooler is included in the design, the weight of this cooler is needed to be calculated. Therefore, without affecting the stability of the forklift, another 165.18 Kg of weight is needed to be removed from the rear axle. Hence, after incorporating the cooler, the new counterweight of the forklift weighs only 239.82 Kg.

To incorporate visual description of the design, components of the forklift are modeled using SolidWorks. *Figure 5.1* shows the overall comparison of the current and new model of the forklift.

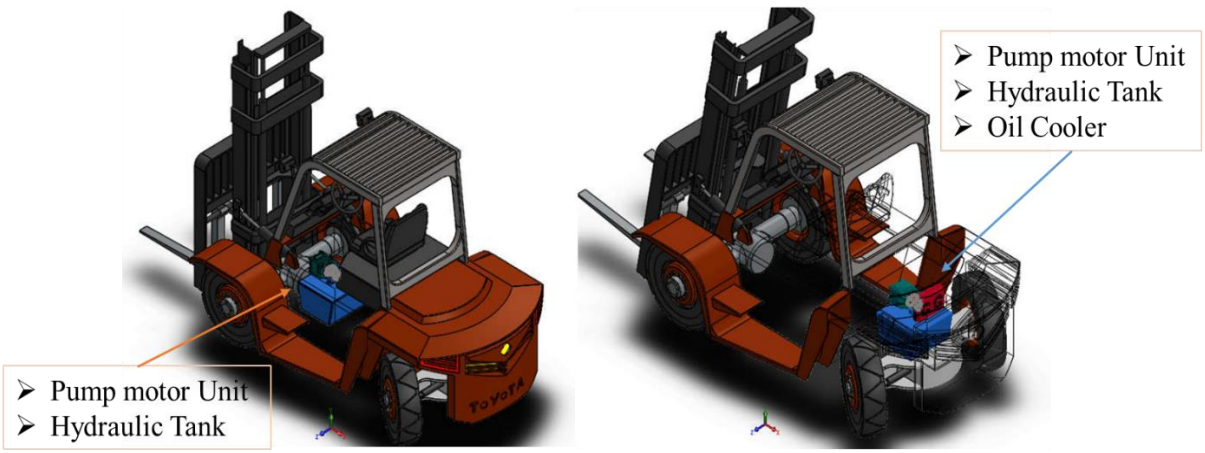

Figure 5.1: Comparison of the current model with the new model of the forklift

The current model has the pump motor unit and hydraulic tank located under the battery, while the new model has them relocated to the rear of the forklift. Moreover, the new model also has an oil cooler incorporated, which is not present in the current model. The relocation of the pump motor unit and hydraulic tank to the rear of the forklift makes it easier to access and service these components.

Table 5.3: Comparison of the current model with the new model of the forklift

Feature	Current Model	New Model
Pump motor unit location	Under the battery	Rear of the forklift
Hydraulic tank location	Under the battery	Rear of the forklift
Oil cooler	Not present	Present
Ease of access to pump motor unit	Difficult	Easy
Ease of access to hydraulic tank	Difficult	Easy
Hydraulic oil	More likely to overheat	Less likely to overheat

Furthermore, the addition of an oil cooler in the new model helps to prevent the hydraulic oil from overheating. This is important, as overheating can damage the hydraulic system and lead to premature failure.

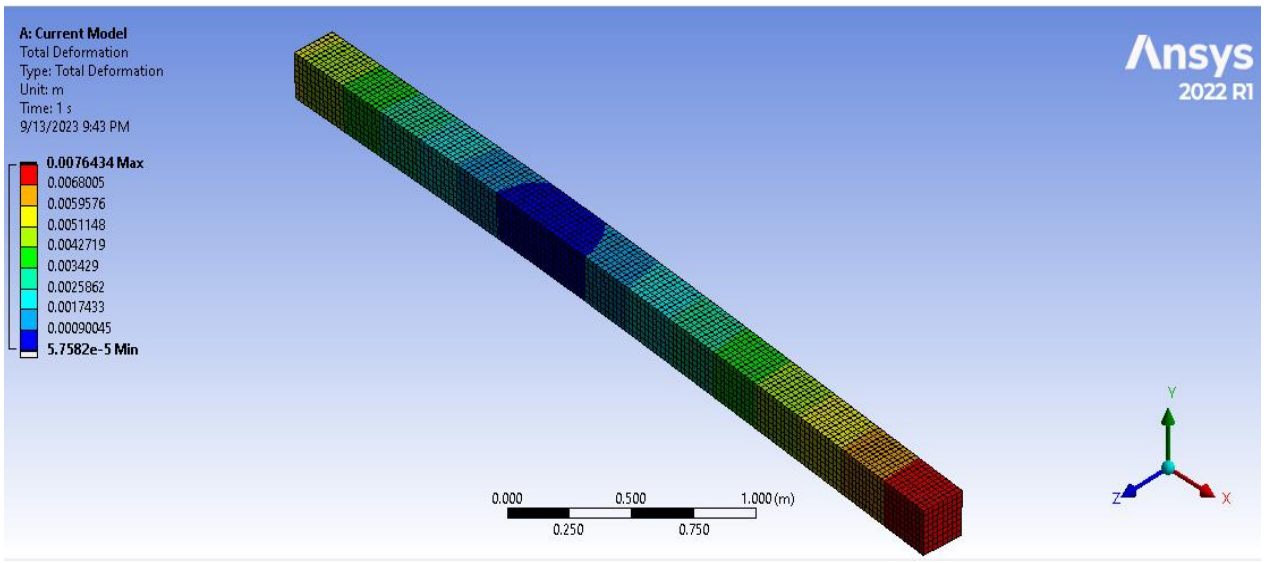

Figure 5.2: The total deformation of the simplified current model of the forklift

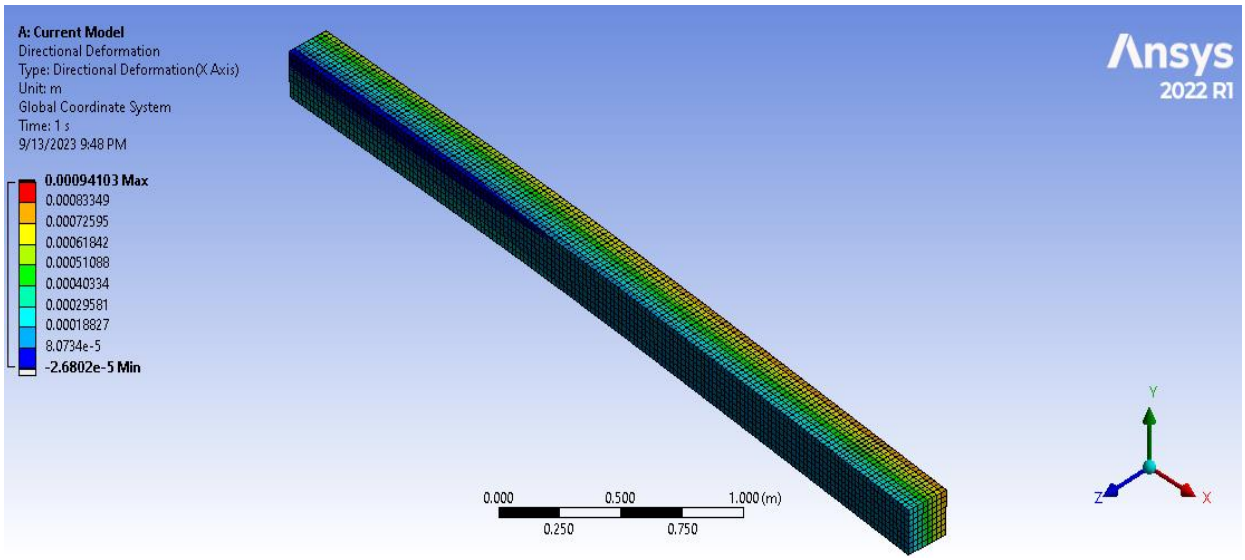

Figure 5.3: The directional deformation of the simplified current model of the forklift

The total deformation of the current model, as shown in *Figure 5.2*, indicates that the counterweight has more deformation about 7.64 mm. However, the deformation on the front axle is low about 0.057 mm. Whereas, the directional deformation of the current model, as

shown in *Figure 5.3*, indicates that the counterweight has more deformation about 0.094 mm. However, the deformation on the front axle is low about 0.0268 mm.

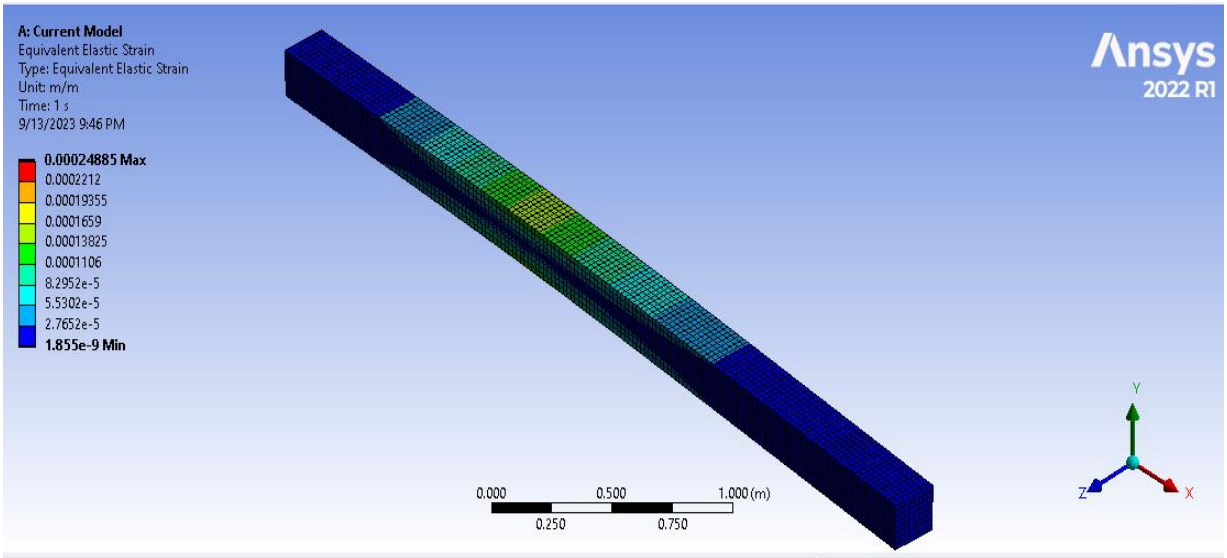

Figure 5.4: The Equivalent Elastic strain of the simplified current model of the forklift

The equivalent elastic strain of the current model, as shown in *Figure 5.4*, indicates that there is more strain on the about 0.025 mm per meter of the length on the middle of the vehicle. However, the strain on the front and rear side of the vehicle are low about 1.85 nm per meter of the length.

The equivalent stress of the current model, as shown in *Figure 5.5*, indicates that there is more strain on the about 49.77 MPa on the middle of the vehicle. However, the stress on the front and rear side of the vehicle are low about 370 MPa.

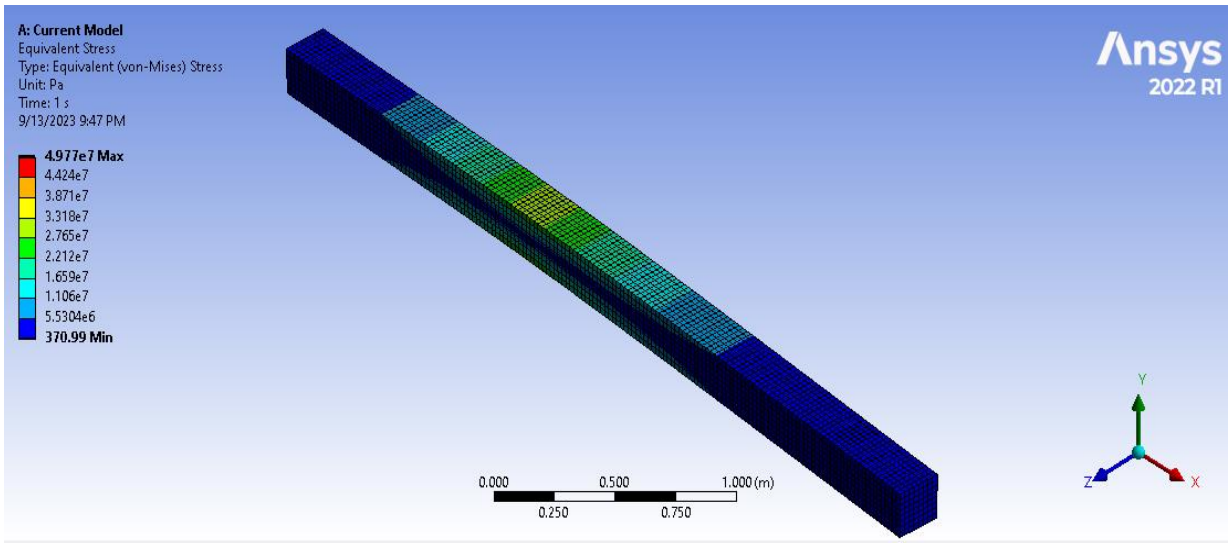

Figure 5.5: The equivalent stress of the simplified current model of the forklift

The total deformation of the new model, as shown in *Figure 5.6*, indicates that the fork has more deformation about 6.1 mm. However, the deformation on the rear axle is low about 0.822 mm. Whereas, the directional deformation of the new model, as shown in *Figure 5.7*, indicates that the counterweight has more deformation about 1.37 mm. However, the deformation on the fork is low about 0.663 mm.

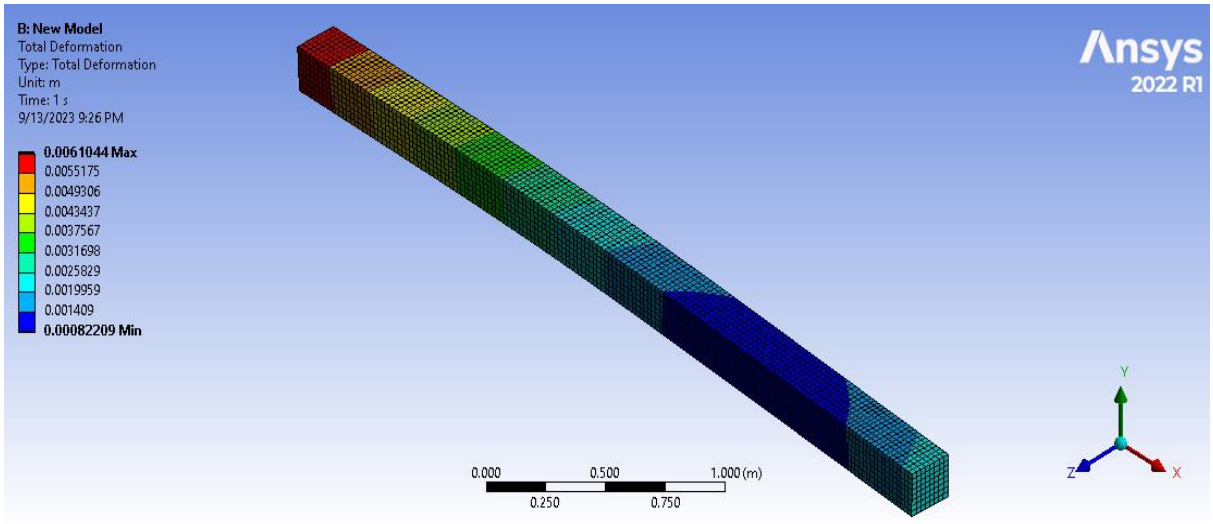

Figure 5.6: The total deformation of the simplified new model of the forklift

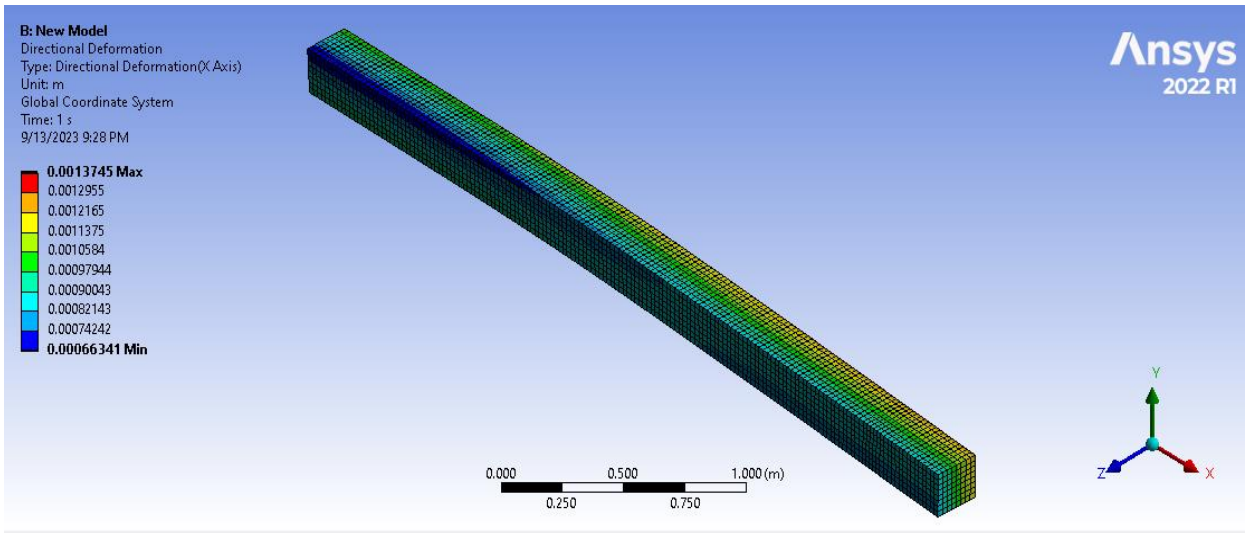

Figure 5.7: The directional deformation of the simplified new model of the forklift

The equivalent elastic strain of the new model, as shown in *Figure 5.8*, indicates that there is more strain on the about 0.0248 mm per meter of the length on the middle of the vehicle. However, the strain on the front and rear side of the vehicle are low about 1.558 nm per meter of the length.

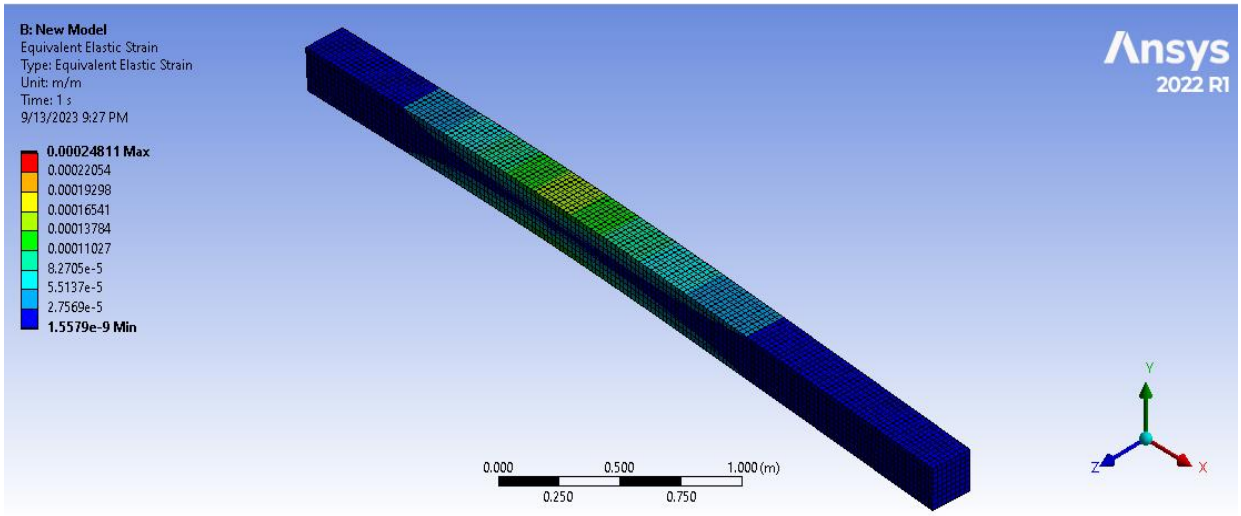

Figure 5.8: The Equivalent Elastic strain of the simplified new model of the forklift

The equivalent stress of the new model, as shown in *Figure 5.9*, indicates that there is more strain on the about 49.62 MPa on the middle of the vehicle. However, the stress on the front and rear side of the vehicle are low about 311 MPa.

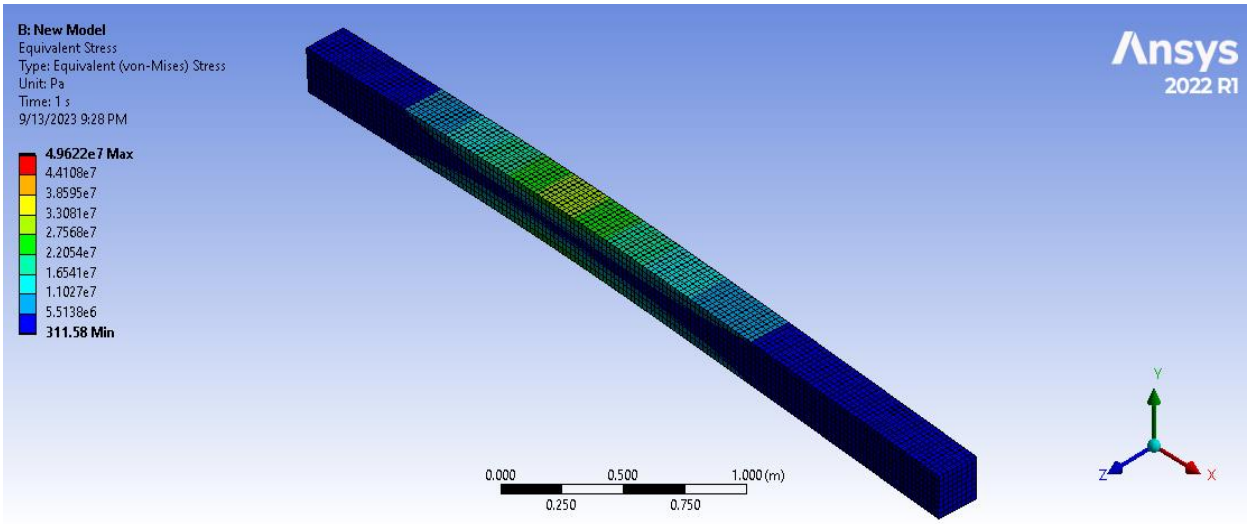

Figure 5.9: The equivalent stress of the simplified new model of the forklift

Table 5.4 summarizes the result obtained from the load and stress analysis of the ANSYS models of both the current forklift model and the new forklift model. The result indicates that, the new model forklift boasts a significant improvement in structural performance compared to the current model. According to ANSYS results, the new model exhibits a lower maximum total deformation at all locations, indicating enhanced rigidity and reduced likelihood of deformation under load. Additionally, the new model showcases a higher minimum total deformation at all locations, suggesting increased stability and a reduced risk of bottoming out under load.

Furthermore, the new model forklift demonstrates a lower maximum directional deformation specifically at the counterweight and fork locations. This implies that the new model is less likely to experience localized deformation when subjected to load. Additionally, the new model showcases a higher minimum directional deformation at the front axle location, further enhancing its stability and reducing the chances of localized deformation under load.

Table 5.4: Comparison of the current and new model forklift based on ANSYS result

Feature or Parameter	Current Model		New Model	
	Location	Value	Location	Value
Maximum total deformation (mm)	Counterweight	7.64	Fork	6.10
Minimum total deformation (mm)	Front Axle	0.0575	Rear Axle	0.82
Maximum Directional deformation (mm)	Counterweight	0.941	Counterweight	1.37
Minimum Directional deformation (mm)	Front Axle	-2.68	Front Axle	0.66
Maximum Elastic strain (mm/m)	Middle body	0.248	Middle body	0.248
Minimum Elastic strain (mm/m)	Front and Rear Axle	$1.85*10^{-6}$	Front and Rear Axle	$1.56*10^{-6}$
Maximum Elastic stress (Pa)	Middle body	$4.97*10^{-7}$	Middle body	$4.96*10^{-7}$
Minimum Elastic stress (Pa)	Front and Rear Axle	371	Front and Rear Axle	312

The new model forklift also exhibits superior resistance to fatigue under load. It showcases a lower maximum elastic strain at the middle body location, indicating a reduced likelihood of plastic deformation. Additionally, the new model displays a higher minimum elastic strain at the front and rear axle locations, enhancing its resistance to fatigue. This resilience to fatigue leads to increased service life, reduced downtime, and improved efficiency.

Chapter Six

6. Conclusion and Recommendation

6.1. Conclusion

Toyota forklifts are some of the most popular and reliable electric forklifts on the market. However, components such as pump motor and oil pump are only accessible after battery is removed from its compartment. Furthermore, since the components are only few centimeters from the floor and the protective device are not installed for them in addition to the unavailability for maintenance, the current placement of pump motor and oil pump of 8FBM 40 Toyota Electric Forklift makes them vulnerable to dirt and water. Thus, it is required to comprehensively analyze and modify the weak points in the design of electric forklift parts that make them susceptible to external factors. Thus, this paper developed a design and a model for relocating the components of the 8FBM 40 Toyota Electric Forklift. The model focuses on the relocation of the pump motor unit with hydraulic pump and hydraulic tank of the forklift for the ease of maintenance and avoiding vulnerability to external factors.

This is done by considering factors such as accessibility of the new location, space availability, weight distribution, vibration generated, and heat dissipation and cooling requirement of the components relocated. Accordingly, the new location with 96.67% of the accessibility score is selected for relocating pump motor unit with hydraulic pump and hydraulic tank to the rear side of the forklift by removing few weights of the counterweight.

Moreover, to increase the lifespan of the hydraulic oil and to reduce the operational cost of the forklift, in addition to relocating the pump motor unit and hydraulic tank, oil cooler is incorporated to the new design. Furthermore, the maximum displacement of the pump motor would be about 0.9994 mm which is within the normal range for a pump motor running at 2280 rpm is within the normal range. Thus, there is no need to worry about premature wear

and tear on the pump motor. In addition, since the new location of the pump rest on the counterweight, it further reduce the effect.

Therefore, it can be concluded that the new model forklift outperforms the current model in terms of accessibility for maintenance, and structural performance. Its superior rigidity and stability, coupled with its resistance to deformation and fatigue, make it a safer and more reliable choice.

6.2. Recommendation

The design and model of the new 8FBM 40 Toyota Electric Forklift model is performed by considering factors such as accessibility of the new location, space availability, weight distribution, vibration generated, and heat dissipation and cooling requirement of the components relocated. However, there may be other factors that may be need to considered. And, in addition ANSYS static structural is used to analyze both the current and new model based on the simplified geometry. Thus, it is recommended that:

- Other design and relocation factors could be considered for further analysis,
- Other software or other ANSYS modules such as LS-DYNA could be considered for comparison purpose, and
- If higher computational capacity is available, using the real model is more accurate than the simplified geometry.

References

Almasi, A. (2017). *Gear Pumps: Design, Operation & Reliability*. https://www.pumpsandsystems.com/gear-pumps-design-operation-reliability

American Industrial Heat Transfer Inc. (2000). *Oil coolers*.

American Industrial Heat Transfer Inc. (2004). *Air Cooled Oil coolers* (Vol. 1, Issue 847).

Borgioli, F., Galvanetto, E., & Bacci, T. (2018). Corrosion behaviour of low temperature nitrided nickel-free, AISI 200 and AISI 300 series austenitic stainless steels in NaCl solution. *Corrosion Science*. https://doi.org/10.1016/j.corsci.2018.03.026

Carvalhal, C. C. (2020). *Safety Optimization of Material Handling Forklift Truck Operations*. KTH Royal Institute of Technology Production.

Cengel, Y. A., & Ghajar, A. J. (2015). *Heat and Mass Transfer - Fundamentals and Applications*. McGraw-Hill Education.

Cheng, L., Zhao, D., Li, T., & Wang, Y. (2021). Modeling and simulation analysis of electric forklift energy prediction management. *7th International Conference on Advances in Energy Resources and Environment Engineering (ICAESEE)*.

Conger. (2023a). *Forklift History: The Complete Story*. https://www.conger.com/forklift-history/

Conger. (2023b). *Toyota Forklift Models: The Complete Guide*. https://www.conger.com/toyota-forklift-models/

darrequipment. (2019). *Electric forklift maintenance basics*. https://darrequipment.com/news/electric-forklift-maintenance-basics/

Doyle, M. G. (2021). *How to safeguard your forklifts in harsh environments*. MHPN. https://www.mhpn.com/article/how_to_safeguard_your_forklifts_in_harsh_environments

Gaines, L. L., Elgowainy, A., & Wang, M. Q. (2008). *Full Fuel-Cycle Comparison of*

Forklift Propulsion Systems.

Gannon, M. (2015). *Hydraulic reservoir design considerations*. Fluid Power World. https://www.fluidpowerworld.com/understanding-hydraulic-reservoir-designs/

H.Liu, S.Kakac, & A.Pramuanjaroenkij. (2012). *Heat exchangers - Selection, rating and thermal design* (Third). CRC Press - Taylor and Francis Group.

Hyster-Yale Materials Handling. (2021). *Regular Forklift Inspections Improve Safety and Productivity*. https://www.hyster.com/ap-region/en-sg/product-solutions/sharing-knowledge/blog/regular-forklift-inspections-improve-safety-and-productivity/

Jönsson, P. (2005). *Procedure for the Reduction of the Effect of Transient Whole Body Vibrations*. Luleå University of Technology.

Lototskyy, M., Parsons, A., Toljan, I., Klochko, Y., Khan, I., Brey, A., Shenker, M., Smith, F., Sita, C., & Linkov, V. (2018). Development and testing of the fuel cell power module for 3-ton electric forklift. *22nd World Hydrogen Energy Conference*.

Ma, L. (2011). *Shock Sensor Detection and Transmission of a Forklift*. Savonia University of Applied Sciences.

Massone, J. M., & Boeri, R. E. (2010). Failure of forklift forks. *Engineering Failure Analysis*, *17*(5), 1062–1068. https://doi.org/10.1016/j.engfailanal.2009.12.005

michael-smith-engineers. (2020). *Useful information on Gear Pumps*. https://www.michael-smith-engineers.co.uk/resources/useful-info/gear-pumps#:~:text=An external gear pump consists,each side of the casing.

Occupational Safety and Health Administration (OSHA). (1999). *Accident Information Bulletin: Control System Failures in Electric-Powered Industrial Trucks*. https://www.osha.gov/shib/12-14-1999_improper_maintenance/

OSHA. (2018). *Occupational Safety and Health Administration*.

Pachakawade, P. M. A., Thakare, A., Kadam, A., Chavhan, A., Kalapad, S., & Pilawan, K.

(2018). *Design and Fabrication of Three Wheeler Drive Forklift for Industrial Warehouses*. *3*(8), 4–6.

powermotiontech. (2023). *Fundamentals of Hydraulic Reservoirs*. https://www.powermotiontech.com/hydraulics/reservoirs-accessories/article/21882642/fundamentals-of-hydraulic-reservoirs

R.K.Shah, & D.P.Sekulic. (2003). *Fundamentals of heat exchanger design*. John Wiley & Sons.

Raut Shubham B, Gawade Karan D., Mane Vinay N., & More Shubham N, S. A. V. (2020). Design of Electric Forklift used in Small industrial Warehouses and Workshops. *International Journal of Engineering Research And*, *9*(04), 734–737. https://doi.org/10.17577/ijertv9is040673

Sachin, S. U., Tushar, S. S., Sachin, S. L., & Prashant, R. K. (2014). Design, Development and Modelling of Forklift. *International Journal of Engineering and Technology*, *3*(4), 1234–1238.

Shanghai Electric Power Company. (2019). *Study on Influence Factors of Lithium Battery Pack Performance of Electric Forklift Trucks*. https://www.researchgate.net/publication/340929504_Study_on_Influence_Factors_of_Lithium_Battery_Pack_Performance_of_Electric_Forklift_Trucks

Shao, Y. (2015). *Design and Analysis of New Flexible and Safe Forklifts*. Boston, Massachusetts : Northeastern University, 2015.

stuffworking. (2023). *Hydraulic Tank Design, Task & Type*. https://stuffworking.com/hydraulic-tank-work/

Summit Toyotalift. (2023). *Mast types and Their Advantages*. https://www.summithandling.com/mast-types-and-their-advantages/

Suryoputro, M. R., Sari, K. D., Sari, A. D., & Widiatmaka, N. W. (2019). Failure Mode and Effect Analysis (Fuzzy FMEA) Implementation for Forklift Risk Management in

Manufacturing Company PT . XYZ. *Materials Science and Engineering*. https://doi.org/10.1088/1757-899X/528/1/012027

Tim O'Brien. (2020). *Assessing the impact of high temperatures on forklifts*. Forkliftaction News.

Toyota. (2022). *Electric Counterbalanced Forklift*. https://www.toyotamaterialhandlingindia.com/products/electric-counterbalanced-forklift.htm

Toyota. (2023). *Productivity Through Innovation and Electricity*. https://www.toyotaforklift.com/lifts/electric-motor-rider-forklifts

Toyota Material Handling. (2023a). *Electric Forklift Advantages & Disadvantages*.

Toyota Material Handling. (2023b). *Electric powered forklift 4.0 - 5.0*.

Toyota Material Handling Company. (2015). *8FBM40, 45, 50 Repair Manual* (pp. 1–776).

University of Southern California. (2010). *A Study of Electric Forklift Failures and Issues*. https://www.usc.edu/acad/eme/farnam-sayed/publications/Printed papers/10asme2.pdf

Vignesh, T., Sudharshan, V., & Survesh, B. (2019). *Design and fabrication of Automatic Industrial Forklift*.

Volland, S. (2021). *Electric Forklifts: The Future of Material Handling Equipment*. MHPN. https://www.mhpn.com/article/electric_forklifts_the_future_of_material_handling_equipment

Wafirulhadi, M., Trisnadewi, T., & Putra, N. (2021). Thermal Management System Based on Phase Change Material (PCM) and Heat Pipe in Lithium-ion Electric Vehicle Batteries. *Journal of Advanced Research in Experimental Fluid Mechanics and Heat Transfer*, *1*(1), 26–35.

Wang, J., Zhao, J., Chu, F., & Feng, Z. (2010). Innovative design of the lifting mechanisms for forklift trucks. *MAMT*, *45*(12), 1892–1896.

https://doi.org/10.1016/j.mechmachtheory.2010.08.002

Wang, Y., Zhao, D., Wang, L., Zhang, Z., Wang, L., & Hu, Y. (2016). Dynamic simulation and analysis of the elevating mechanism of a forklift based on a power bond graph. *Journal of Mechanical Science and Technology*, *30*(9), 4043–4048. https://doi.org/10.1007/s12206-016-0817-y

Wu, J., Zhou, X., Vo, T. P., & J., Z. (2021). The Influence of Low Cycle Fatigue on Load Carrying Capacity of Mast in Electric Forklift. *International Journal of Advanced Manufacturing Technology*, *117*(4), 139–149.

Yadav, J., Vishwakarma, M., Shakir, S. M., Yadav, S., & Rehman, Y. (2022). Design and Fabrication of Electric Forklift. *International Journal for Research in Applied Science & Engineering Technology*, *10*(IV), 589–593.

Yao, W., Dingxuan, Z., Lei, W., Lili, W., & Yanjuan, H. (2015). Analysis of New Type Elevating Mechanism for Hybrid Forklift Based on ANSYS. *5th International Conference on Advanced Design and Manufacturing Engineering (ICADME 2015)*, 247–250.

Yao, Z., Li, H., & Zhou, L. (2022). *Research and Development of Electric Power Lifting Truck*. https://doi.org/10.1088/1742-6596/2218/1/012076

Zhao, H., Deng, W., Li, G., & Yin, L. (2017). Research on a new fault diagnosis method based on WT, improved PSO and SVM for motor. *Fault Diagnosis*, *9*(4), 289–298. https://doi.org/10.2174/2212797609666161018164249

Appendix

Appendix 1: Basic Dimensions of 8FBM 40 Toyota Electric Forklift

Truck specifications					8FBMT40
Identification	1.1	Manufacturer			Toyota
	1.2	Model			8FBMT40
	1.3	Drive			Electric
	1.4	Operator type			Rider seated
	1.5	Load capacity/rated load	Q	kg	4000
	1.6	Load centre	c	mm	500
	1.8	Load distance, centre of drive axle to fork	x	mm	518
	1.9	Wheelbase	y	mm	2030
Weight	2.1	Service weight		kg	6556
	2.2	Axle load, with load, front/rear		kg	9555 / 1102
	2.3	Axle load, without load, front/rear		kg	3558 / 3099
Tyres	3.1	Tyre: C = Cushion, SE = Super elastic, PN = Pneumatic, TW = Twin			SE
	3.2	Tyre size, front			250-15
	3.3	Tyre size, rear			23x9-10
	3.5	Wheels, number front/rear (x = driven wheels)			2 / 2
	3.6	Track width, front	b_{10}	mm	1119
	3.7	Track width, rear	b_{11}	mm	1113
Dimensions	4.1	Tilt of mast/fork carriage forward/backward	α/β	deg	5/10
	4.2	Height, mast lowered	h_1	mm	2500
	4.3	Free lift	h_2	mm	130
	4.4	Lift	h_3	mm	3300
		Lift height	h_{23}	mm	3350
	4.5	Height, mast extended	h_4	mm	4156
	4.7	Height of overhead guard (cab)	h_6	mm	2360
	4.8	Seat height/stand height	h_7	mm	1277
	4.12	Coupling height	h_{10}	mm	550
	4.19	Overall length	l_1	mm	3907
	4.20	Length to face of forks	l_2	mm	2907
	4.21	Overall width	b_1	mm	1345
	4.22	Fork dimensions	s/e/l	mm	50/150/1000
	4.23	Fork carriage DIN 15 173, class/type A, B			IIIA
	4.24	Fork-carriage width	b_3	mm	1170
	4.31	Ground clearance, with load, below mast	m_1	mm	150
	4.32	Ground clearance, centre of wheelbase	m_2	mm	152
	4.33	Aisle width for pallets 1000x1200 crossways	A_{st}	mm	4260
	4.34	Aisle width for pallets 800x1200 lengthways	A_{st}	mm	4460
	4.35	Turning radius	W_a	mm	2543
	4.36	Internal turning radius	b_{13}	mm	685

Performance data	5.1	Travel speed, with/without load		km/h	18/18
	5.2	Lift speed, with/without load		m/s	0,35/0,46
	5.3	Lowering speed, with/without load		m/s	0,55/0,46
	5.5	Drawbar pull, with/without load		N	12420
	5.6	Max. drawbar pull, with/without load		N	22000
	5.7	Gradeability, with/without load		%	11,3/17
	5.8	Max. gradeability, with/without load		%	15/25
	5.9	Acceleration time, with/without load		s	5,1/4,5
	5.10	Service brake			Mechanical/hydraulic
Electric motor	6.1	Drive motor rating S2 60 min		kW	25,2
	6.2	Lift motor rating S3 15%		kW	25,5
	6.3	Battery acc. to DIN 43 531/35/36 A, B, C, no			43536
	6.4	Battery voltage, nominal capacity K_5		V/Ah	80 / 840
	6.5	Battery weight		kg	2178
	6.6	Energy consumption acc. to EN16796:2016		kWh/h	9.8
Other	8.1	Type of drive control			AC
	8.2	Operating pressure for attachments		bar	160-180
	8.3	Oil volume for attachments		l/min	70
	8.4	Sound level at the driver's ear according to EN 12 053		dB(A)	68

Appendix 1: Basic Dimensions of 8FBM 40 Toyota Electric Forklift